

Forecasting 3-D fish movement behavior using a Eulerian–Lagrangian–agent method (ELAM)

R. Andrew Goodwin^{a,*}, John M. Nestler^{b,1}, James J. Anderson^{c,2},
Larry J. Weber^{d,3}, Daniel P. Loucks^{e,4}

^a *Civil & Environmental Engineering, Cornell University, Environmental Laboratory, U.S. Army Engineer Research & Development Center, CENWP-EC-HD, 333 SW 1st Ave., P.O. Box 2946, Portland, OR 97208 (US mail)/97204 (courier), USA*

^b *Environmental Modeling & System-wide Assessment Center, U.S. Army Engineer Research & Development Center, CEERD-IV-Z, 3909 Halls Ferry Rd., Vicksburg, MS 39180-6199, USA*

^c *School of Aquatic & Fishery Sciences, University of Washington, Columbia Basin Research, 1325 4th Ave., Suite 1820, Seattle, WA 98101, USA*

^d *IHR—Hydroscience & Engineering, University of Iowa, 100 Stanley Hydraulics Laboratory, Iowa City, IA 52242-1585, USA*

^e *Civil & Environmental Engineering, Cornell University, 311 Hollister Hall, Ithaca, NY 14853-3501, USA*

Received 19 February 2004; received in revised form 26 July 2005; accepted 1 August 2005

Available online 23 September 2005

Abstract

We describe a Eulerian–Lagrangian–agent method (ELAM) for mechanistically decoding and forecasting 3-D movement patterns of individual fish responding to abiotic stimuli. A ELAM model is an individual-based model (IBM) coupling a (1) Eulerian framework to govern the physical, hydrodynamic, and water quality domains, (2) Lagrangian framework to govern the sensory perception and movement trajectories of individual fish, and (3) agent framework to govern the behavior decisions of individuals. The resulting ELAM framework is well suited for describing large-scale patterns in hydrodynamics and water quality as well as the much smaller scales at which individual fish make movement decisions. This ability of ELAM models to simultaneously handle dynamics at multiple scales allows them to realistically represent fish movements within aquatic systems. We introduce ELAMs with an application to aid in the design and operation of fish passage systems in the Pacific Northwest, USA.

* Corresponding author. Tel.: +1 503 808 4872; fax: +1 503 808 4875.

E-mail addresses: rag12@cornell.edu (R.A. Goodwin), john.m.nestler@erdc.usace.army.mil (J.M. Nestler), jim@cbr.washington.edu (J.J. Anderson), larry-weber@uiowa.edu (L.J. Weber), DPL3@cornell.edu (D.P. Loucks).

¹ Tel.: +1 601 634 2720; fax: +1 601 634 3129.

² Tel.: +1 206 543 4772; fax: +1 206 616 7452.

³ Tel.: +1 319 335 5597; fax: +1 319 335 5238.

⁴ Tel.: +1 607 255 4896; fax: +1 607 255 9004.

Individual virtual fish make behavior decisions about every 2.0 s. These are sub-meter to meter-scale movements based on hydrodynamic stimuli obtained from a hydraulic model. Movement rules and behavior coefficients are systematically adjusted until the virtual fish movements approximate the observed fish.

The ELAM model introduced in this paper is called the Numerical Fish Surrogate. It facilitated the development of a mechanistic biological-based hypothesis describing observed 3-D movement and passage response of downstream migrating juvenile salmon at 3 hydropower dams on 2 rivers with a total of 20 different structural and operational configurations. The Numerical Fish Surrogate is presently used by the U.S. Army Corps of Engineers and public utility districts during project planning and design to forecast juvenile salmon movement and passage response to alternative bypass structures.

Published by Elsevier B.V.

Keywords: Fish; Movement rules; Individual-based model; Eulerian; Lagrangian; Agent; Behavior

1. Introduction

Understanding movements of individuals is important for understanding population dynamics (Turchin, 1998). Identifying underlying mechanisms that influence spatial patterns in populations improves forecasts (Harte, 2002) of alternative management strategies on the spatial dynamics of populations critical for assessing and managing fisheries (Schmalz et al., 2002; Pelletier and Parma, 1994) and improving water resource management (Van Winkle et al., 1993). In many systems, the spatial pattern of individuals is driven by environmental factors (Pientka and Parrish, 2002), which can be evaluated separately from biological interactions (Hussko et al., 1996; Pientka and Parrish, 2002).

The need to understand fish movements is particularly acute in the Columbia–Snake River system in the Pacific Northwest of the United States where tens of millions of juvenile salmon and steelhead (migrants) migrate downstream through eight dams. This migration consists of dozens of runs, of which 12 are listed under the Endangered Species Act. Since migrants passing through turbines may experience significant mortality (5–15%) research efforts over several decades have been devoted to diverting migrants over spillways and through bypass systems. However, bypass systems have achieved only limited and variable success (Coutant and Whitney, 2000) at considerable cost. Anderson (1988) first proposed using hydrodynamic and behavior information to design bypass systems. Anderson (1991) introduced the first such mathematical model. However, until recently no model has been sufficiently accurate to be of value in engineering design of bypasses.

Tools needed to understand and model fish movements in response to environmental cues are now

available. Advances in telemetry (e.g., Steig, 1999; Gerolotto et al., 1999; Johnson et al., 1999; Lucas and Baras, 2000) can provide high-resolution 3-D tracks of individual movements. Computational fluid dynamics (CFD) models can now describe hydrodynamic patterns at scales meaningful to fish, and laboratory studies have defined many sensory abilities of fish to distinguish elements of hydrodynamic fields (e.g., Coombs et al., 2001; Kröther et al., 2002). However, mathematical methods linking fish trajectories to hydrodynamic patterns in terms of fish sensory and behavioral elements remain a challenge (Steel et al., 2001). We describe an integrated mathematical method that couples a (1) Eulerian framework for describing the physical and hydrodynamic domain of a hydropower dam forebay, (2) Lagrangian framework for describing the sensory perception and movement trajectories of individual fish, and (3) agent framework for describing the changes in swimming behavior of individual fish responding to stimuli. Together these coupled elements comprise a Eulerian–Lagrangian–agent method (ELAM) model to mechanistically decode and forecast movement of downstream outmigrating juvenile salmon (migrants) as they approach and pass hydropower dams of the Columbia and Snake Rivers of the Pacific Northwest.

2. Model overview

2.1. Describing hydrodynamic pattern with the Eulerian framework

Understanding migrant responses to hydrodynamic patterns close (<10 m) to a bypass entrance is critical

to understanding and improving bypass performance (Johnson et al., 2000). Features of bypass structures (Fig. 1) have scales of sub-meters to meters. In the ELAM model for migrants, the Numerical Fish Surrogate, the Eulerian framework consists of a mesh made up of discrete points (nodes) describing the physical domain of the dam forebay. Hydrodynamic patterns are calculated by a computational fluid dynamics (CFD) model that solves the Navier–Stokes equations of fluid motion at discrete points in the Eulerian mesh. We use the 3-D “Unsteady, Unstructured Reynolds-Averaged Navier–Stokes” (U^2 RANS) CFD model (Lai et al., 2003a,b; Lai, 2000) to describe the hydrodynamic patterns in the forebays of three hydropower dams (Fig. 2).

2.2. Describing sensory perception with the Lagrangian framework

Hydrodynamic information generated at discrete points in the Eulerian mesh may be interpolated to locations anywhere within the physical domain where fish may be. This conversion of information from the Eulerian mesh to a Lagrangian framework allows the generation of directional sensory inputs and movements in a reference framework similar to that perceived by real fish. Movement is treated as a two-step process: first, the fish evaluates agent attributes within the detection range of its sensory system and, second, it executes a response to an agent by moving (Bian, 2003). The volume from which a fish acquires

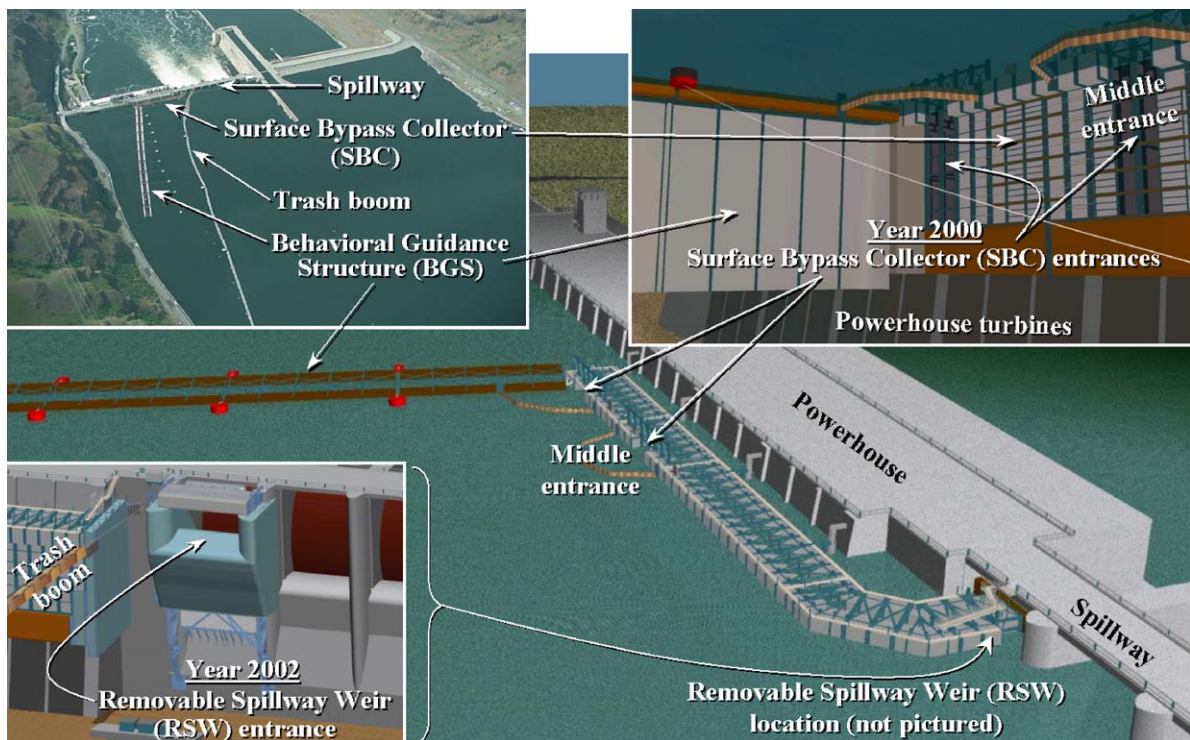


Fig. 1. Illustration of two different migrant bypass structures at Lower Granite Dam on the Snake River, WA USA. In 2000, the Surface Bypass Collector (SBC) was deployed. In 2002, the Removable Spillway Weir (RSW) was deployed. The Behavioral Guidance Structure (BGS) is intended to guide migrants into the bypass (SBC or RSW). The BGS is a suspended steel wall approximately 24.4 m deep at its intersection with the powerhouse and tapers in step-wise manner to a minimum of 16.8 m at its upstream end. The trash boom is approximately a constant 1.2 m deep. The BGS and trash boom were present for both 2000 and 2002 field studies. *Note:* both the SBC (in 2000) and the RSW (in 2002) occupied the spillbay nearest the powerhouse. In 2002, the SBC was not operated and the conduit connecting the dormant SBC to the spillbay was removed in lieu of the RSW.

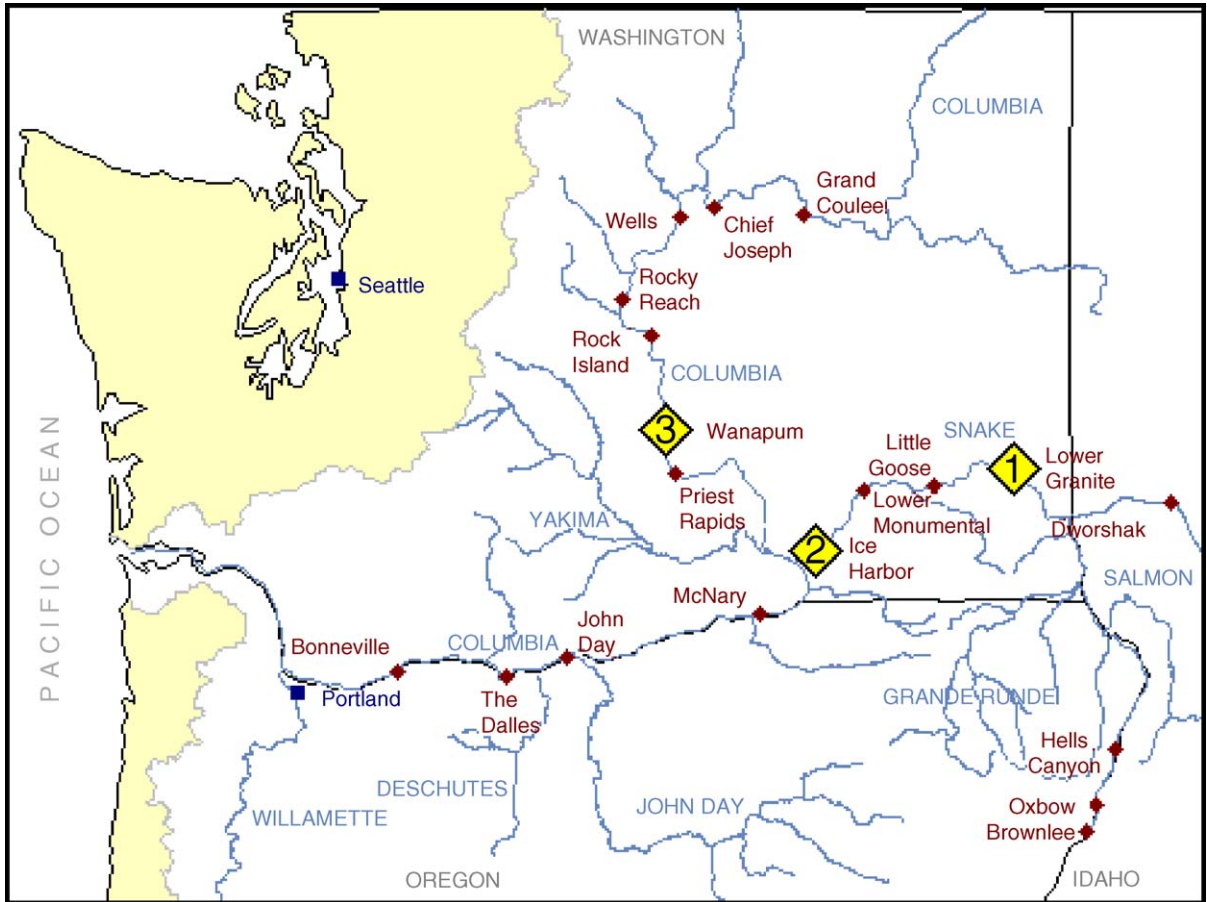


Fig. 2. Map of the Pacific Northwest USA showing the locations of three hydropower dams with Numerical Fish Surrogate applications: (1) Lower Granite, (2) Ice Harbor, and (3) Wanapum.

decision-making information is represented as a sensory ovoid (Fig. 3). A virtual fish's sense of direction in each time increment is based on its orientation at the beginning of the time increment. Directional sensory inputs are tracked relative to the horizontal orientation of the fish because fish response to laterally-located versus frontally-located stimuli can be different (Coombs et al., 2000). The sensory ovoid has a vertical reference because fish detect accelerations and gravitation through the otolith of its inner ear (Paxton, 2000). It also senses three-dimensional information on motion (Braun and Coombs, 2000). In the Numerical Fish Surrogate, we use a symmetrical (spherical) sensory ovoid for migrants although it can be either symmetrical or distorted (Fig. 3) (Goodwin et al., 2001; Nestler et al., 2002).

The scale of the sensory ovoid represents the sensory range of the fish lateral line mechanosensory system. Sensory Query Distances (SQDs) characterize the range of the sensory ovoid from the fish centroid parallel (SQD_x), perpendicular (SQD_y), and vertical (SQD_z) to the long axis of the fish (Fig. 3). The detection range of the lateral line mechanosensory system and, therefore SQDs, is a function of fish length (Coombs, 1999). Longer fish are able to detect hydrodynamic stimuli from greater distances (Denton and Gray, 1983, 1988, 1989; Kalmijn, 1988, 1989; Coombs, 1996, 1999). With respect to prey items, the "active space" of the lateral line system is 1–2 body lengths but the actual range depends on a number of factors including size and form of the disturbance source (Coombs, 1999).

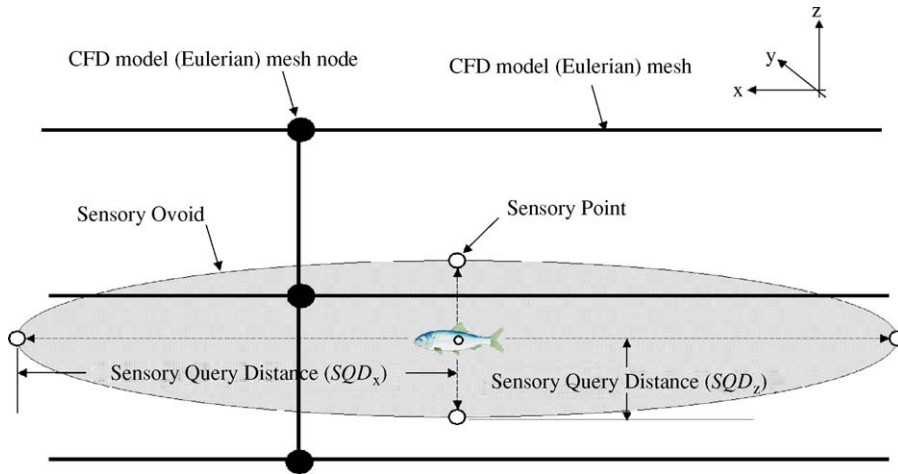


Fig. 3. Two-dimensional view (longitudinal and vertical) of a virtual fish computational sensory ovoid. The sensory ovoid is independent of the Eulerian mesh topology. Sensory points that exceed the physical domain, i.e., when the fish is near the domain boundary, may be repositioned at the boundary or flagged as ‘out-of-bounds’.

The SQD is composed of two metrics: biological sensory query distance (SQD_b) and CFD model sensory query distance (SQD_{CFD}). SQD_b is related to model time increment Δt (s), fish body length S_f (m), and operating range of the fish sensory system to the agent in a 1.0-s time increment D_a (body lengths) calculated as:

$$SQD_b = \Delta t \cdot S_f \cdot D_a \quad (1)$$

Resolution of the Eulerian model or field data can limit the usefulness of SQD_b . Frequently, resolution of mesh-based data is insufficient to calculate gradient information with significant precision using only a distance of SQD_b . Therefore, a larger distance (SQD_{CFD}) is required to estimate gradient information. SQD_{CFD} is based on resolution of the mesh-based data and interpolation scheme used. SQD_{CFD} may change based on the position of the virtual fish in the Eulerian mesh since some areas are often gridded more densely, i.e., provide higher resolution of modeled data. SQD is selected for each fish at every time step as:

$$SQD = \max\{SQD_b, SQD_{CFD}\} \quad (2)$$

The SQD may be modified to reflect factors such as fish physiological condition, time of day, water quality, and whether the fish swims alone or is part of a school. To capture environmental gradients at multiple spatial

scales, SQD values fluctuate randomly each time increment according to a user-defined percentage, as suggested by Railsback et al. (1999a) and Goodwin et al. (2001). In the Numerical Fish Surrogate, the spherical dimension of the sensory ovoid, SQD, for migrants is based on a 2.0-s time increment, 0.2 m migrant length, and a hydrodynamic agent detection range of 2 body lengths for a 1.0-s time increment. The biological sensory query distance (SQD_b) is 0.8 m, but SQD_{CFD} was determined through trial and error to be approximately 1.25 m. To capture gradients at more than one spatial scale, SQD fluctuates each separate time increment to a value between 1.25 m and 150% of 1.25 m (1.875 m). Larger fluctuations can be used but at the expense of additional sensory point domain boundary violations.

2.3. Describing movement with the Lagrangian framework

Movement may be classified by whether incremental movement length (speed) and direction are interdependent or independent (Wu et al., 2000; Marsh and Jones, 1988). Behavior rules in the Numerical Fish Surrogate produce a 3-D volitional swimming vector in which speed and orientation are determined interdependently for each fish at every 2.0-s increment. The resultant volitional fish swim vector is then decomposed into Cartesian vector components (u_f , v_f , w_f)

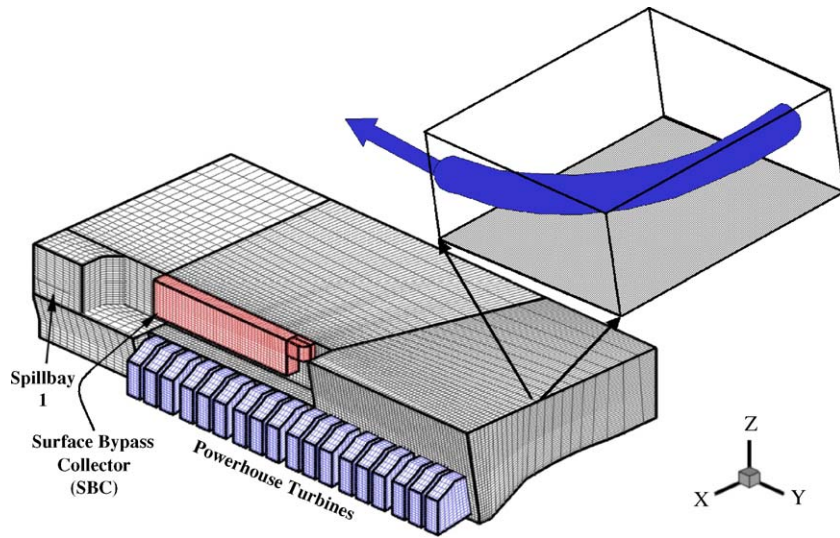


Fig. 4. Eulerian mesh discretization of the Lower Granite Dam forebay near the powerhouse structure (Fig. 1). *Inset*: conceptually dispensing with the arbitrary Eulerian mesh orientation by defining a supplemental Lagrangian reference frame oriented uniquely for each fish at every time step.

coinciding with the axes of the Eulerian mesh (Fig. 4). These vectors are added to the flow vectors (u, v, w) interpolated to the fish's location to update the coordinates (x_t, y_t, z_t) at time t from the previous position ($x_{t-1}, y_{t-1}, z_{t-1}$) after time increment (Δt) as:

$$x_t = x_{t-1} + (u + u_f) \cdot \Delta t \quad (3)$$

$$y_t = y_{t-1} + (v + v_f) \cdot \Delta t \quad (4)$$

$$z_t = z_{t-1} + (w + w_f) \cdot \Delta t \quad (5)$$

Simulating the continuous (Lagrangian) movement of individuals in a (Eulerian) mesh of discrete points is difficult and has limited the use of integrated Eulerian–Lagrangian methods (ELMs) in individual-based modeling (Bian, 2003). For example, existing 3-D fluid and water quality dynamics models may use any one of a number of different Eulerian mesh topologies including multi-block, near-orthogonal structured, unstructured hexahedral, unstructured tetrahedral, mixed hexahedral–tetrahedral, or other mesh topologies using arbitrarily shaped cells (e.g., Lai et al., 2003a,b; Lai, 2000). Computationally efficient simulation of many virtual individuals in large physical domains, such as a dam forebay, with moderate-to-high mesh resolution requires sophisticated parallel particle-

tracking algorithms (e.g., Cheng and Plassmann, 2001, 2002, 2004; Cheng et al., 2004) compatible with different mesh topologies. These particle-tracking algorithms must be supplemented with efficient mesh search and interpolation algorithms (e.g., Khoshniat et al., 2003) and bookkeeping schemes before ELMs can be used in individual-based models (IBMs).

The current form of the Numerical Fish Surrogate uses a particle-tracking algorithm compatible with many mesh topologies. For brevity, we limit our discussion to multi-block, near-orthogonal structured meshes (Fig. 4). The particle-tracking algorithm for multi-block, near-orthogonal structured meshes first converts the mesh discretization of the 3-D physical domain from Cartesian to contravariant space (Fig. 5). All 3-D cells are translated to unit size, i.e., $1 \times 1 \times 1$, and vector quantities are appropriately scaled. Second-order interpolation schemes are used to maintain accuracy in the spatial derivatives of the Eulerian mesh data. The position of an individual in contravariant space is tracked by displacement within the cell (i.e., the unit cube) and the Cartesian position of the reference node of the cell (Fig. 6). The individual's position in contravariant space efficiently identifies nearest points in the Eulerian mesh where agent attributes from the CFD model are available for interpolation.

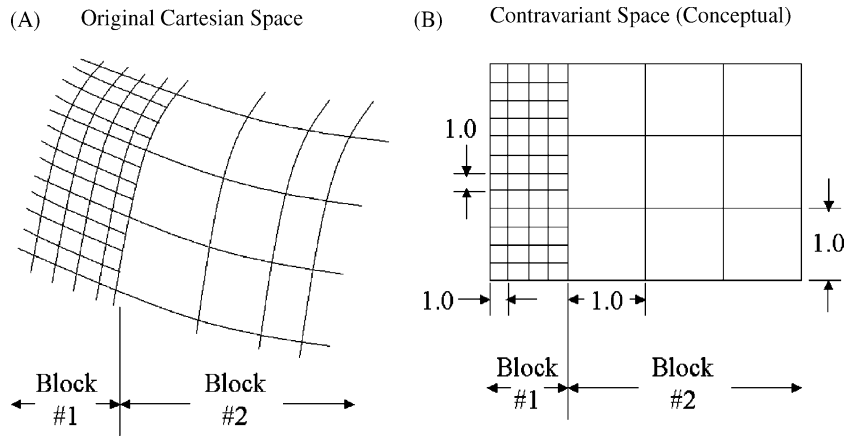


Fig. 5. Comparison of a multi-block, near-orthogonal structured mesh (2-D) in original Cartesian space (A) and then in (conceptual) contravariant space (B). All vector quantities are appropriately scaled in contravariant space to maintain conservation principles.

Variables in Eqs. (3)–(5) are converted from Cartesian to contravariant form to update an individual’s position. Since contravariant space consists of unit cubes, computations are highly efficient although computational costs occur as the simulation alternates between Cartesian and contravariant forms.

2.4. Describing sensory processing and behavior decisions with the agent framework

Models of animal behavior range from the complex, in which swimming is defined as the interactions of muscles and neurons (Terzopoulos et al., 1995; Ijspeert

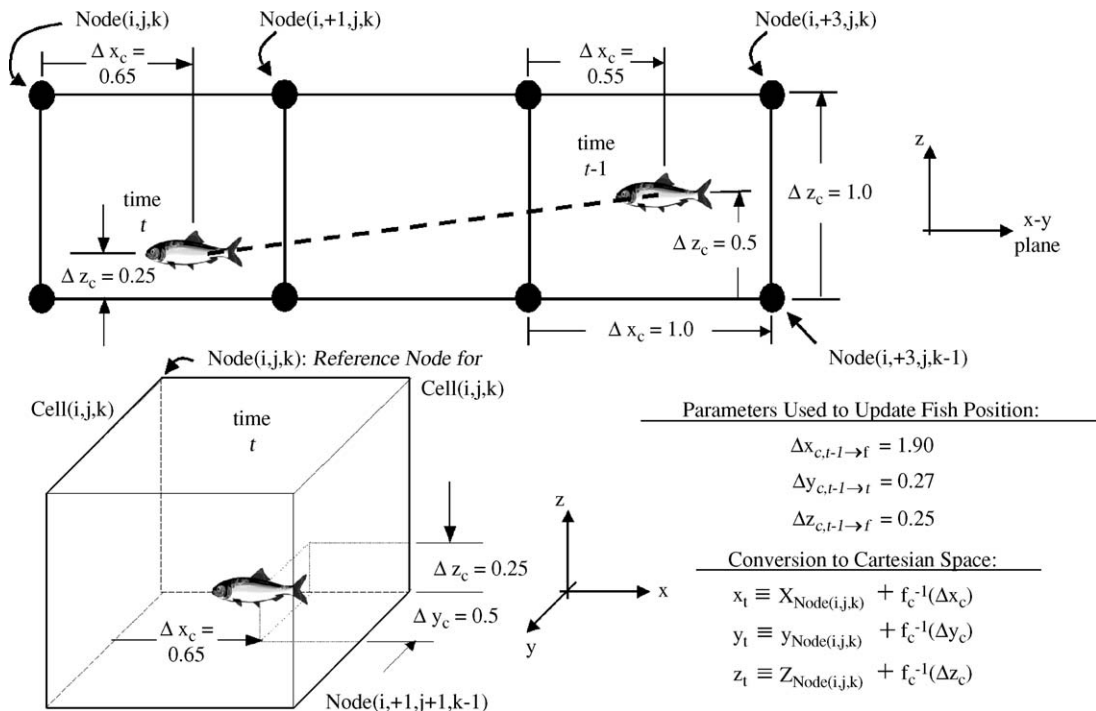


Fig. 6. Bookkeeping individual virtual fish movement in contravariant space. f_c^{-1} is the inverse function for converting contravariant displacements within a unit cube into Cartesian space displacements for graphical output and movement analysis.

and Kodjabachian, 1999) to rule-based methods such as the barrier avoidance rule Haefner and Bowen (2002) applied to fish moving through the velocity field of a diversion structure. In our system, fish move through the forebay of a large hydropower dam and respond only to hydrodynamic cues generated by forebay structures without visual or tactile contact with solid structures.

2.4.1. Identifying a mechanistic biological movement hypothesis

Through natural selection riverine fish have evolved rheotactic behaviors in response to a detailed perception of the hydrodynamic environment (Kalmijn, 2000). Although what a fish perceives is undoubtedly complex, we hypothesize salient hydraulic cues driving their behaviors by considering hydrogeomorphology, the Navier–Stokes equation of fluid motion and fish sensory capabilities. Aquatic environments are rich in acoustic and hydrodynamic signals (Schilt and Nestler, 1997; Rogers and Cox, 1988) because any object that moves relative to a fluid generates a disturbance field (Montgomery et al., 1995). Fish can detect flow strength and direction (Montgomery et al., 2000; Voigt et al., 2000), hydraulic strain (steady-state acceleration) (Hudspeth, 1989), whole body acceleration (Kalmijn, 1989), and migrants are sensitive to pressure (Coutant, 2001). Water velocity, its first derivatives of strain and acceleration, and pressure are also components of the Navier–Stokes equation of fluid motion. We use the hydraulic variables of the strain–velocity–pressure (SVP) Hypothesis in the Numerical Fish Surrogate described in Goodwin (2004). The strain and velocity components of the SVP Hypothesis are best explained in the context of river geomorphology. In free flowing streams, flow pattern results from: (1) friction resistance producing wall-bounded flow gradients occurring when a solid boundary (e.g., river channel) exerts friction force on moving water and (2) form resistance producing free-shear flow gradients occurring when an obstruction in the flow (e.g., stump or rock outcrop projecting into the flow field) produces a local constriction in flow area. These two patterns provide cues to migrating fish about spatial patterns allowing them to navigate through complex flow fields. Information contained in the hydraulic strain and velocity fields is sufficient to separate structures producing friction resistance and form resistance flows (Goodwin,

2004). Wall-bounded flow gradients, associated with friction resistance, exhibit increasing hydraulic strain and decreasing water velocity towards a solid boundary. Free-shear flow gradients, associated with form resistance, exhibit increasing strain and water velocity as an obstruction is approached. The pressure component of the SVP Hypothesis recognizes that migrants generally change depth at a rate related more to their ability to adjust swim bladder volume than their vertical swimming velocity. Within the Numerical Fish Surrogate, we consider these hydrodynamic cues to be environmental agents that interact with the fish agent.

The SVP Hypothesis uses four agents: the default (A_0) occurs in the absence of other agents, wall-bounded flow gradient (A_1), free-shear flow gradient (A_2), and pressure gradient (A_3). A fish perceives an agent by its hydraulic signature. A wall-bounded flow gradient is perceived when a strain threshold, k_1 , is exceeded. A free-shear flow gradient is perceived when a strain threshold, k_2 , is exceeded where $k_2 \gg k_1$. An excessive change in pressure is perceived when the change in depth, associated with hydrostatic pressure, exceeds threshold k_3 .

We represent the perceived stimuli strength of strain at the fish centroid at time t following an analogy to the decibel scale for sound. This assumes the fish's perception of total strain, $I(t)$, is not linear with its physical intensity, $S(t) = \sum |\partial u_i / \partial u_j|$, but rather its log. A reference value, S_0 , is used to scale perceived strain so increasing physical intensity, $S(t)$, corresponds to increasing $I(t)$:

$$I(t) = \log_{10} \left[\frac{S(t)}{S_0} \right] \quad (6)$$

We hypothesize that an individual's ability to detect when a strain threshold is exceeded is similar to Weber's Law (1846), which states that the "just noticeable difference" between a signal and the background stimuli is a constant fraction of the background stimuli intensity. Mathematically, the detection of a threshold is expressed as:

$$\frac{I(t)}{I_a(t)} > k_i \quad (7)$$

where I_a is the perceived background or acclimated strain level, k_i is the threshold level associated with A_i . Eq. (7) implies that a larger change in strain intensity is needed to identify the presence of the agent at

higher background levels than at lower levels and that identification depends intimately on the individual's antecedent experience. Implicit in each threshold is a time scale over which the change occurs.

Since $I(t)$ is the instantaneous perceived total hydraulic strain, the acclimated level is represented by a moving average as:

$$I_a(t) = (1 - m_{\text{strain}}) \cdot I(t) + m_{\text{strain}} \cdot I_a(t - 1) \quad (8)$$

where m_{strain} is an adaptation coefficient with a value between 0 and 1 that adjusts how information from the present combines with information from the past. Eq. (8) is an exponential moving average having a long history in psychology studies (Bush and Mosteller, 1955). Variable discounting of past information is consistent with the approach described in Hirvonen et al. (1999). Our method applies exponential moving averages to physicochemical stimuli and is supported by observations of juvenile chum salmon, whose thermal tolerance and resistance is influenced by prior thermal history (Birtwell et al., 2003; Brett, 1952).

We represent the migrant's perception of pressure as linear with the physical intensity of hydrostatic pressure, which is proportional to depth. We use a linear difference between instantaneous, $d(t)$, and acclimated, $d_a(t)$, depths for detecting pressure gradient threshold k_3 . Acclimated depth is calculated using Eq. (8) by replacing perceived strain with depth and identifying a separate adaptation coefficient m_{depth} .

The algorithm allows a virtual migrant to identify one of the four agents, each of which elicits a specific behavior (Table 1): (B_0) swimming with the flow vector, (B_1) swimming towards increasing water velocity to minimize strain, (B_2) swimming towards decreasing water velocity or against the flow vector to minimize strain, and (B_3) swimming towards acclimated pressure (depth). Swimming speed is bounded above by a burst speed of approximately 10 body lengths per second and below by the nominal cruising speed of approx-

imately 2 body lengths per second (Beamish, 1978). Fish orientation and speed for each time increment are described by the specified behavior B_i plus a random component.

2.4.2. Converting identification of an agent into a neurological response

We have shown how a fish could associate stimuli inputs with specific agents, A_i , according to whether or not the signals exceed intensity levels k_i . However, converting identification of an agent into a neurological response to that agent is not straightforward. Workman et al. (2002) describe the probability of initiation of upstream migration of steelhead as a power function of the difference between temperature and a threshold. However, in our case, and in general, animals have a multitude of time varying streams of information and must select between numerous behaviors. Hence, a one-to-one relationship between a behavior and a stimulus is not adequate. To characterize how a fish responds to multiple streams of information we use a game theoretic framework adapted by Anderson (2002). In this framework, each behavior has an associated intrinsic utility (u_i). The animal estimates the probability (P_i) of obtaining the utility from the information stream. We treat information acquisition as discrete events because our model updates the system state in discrete increments of time. Because there may be a bioenergetic cost (C_i) in carrying out the behavior, independent of whether or not the utility is obtained, the expected utility (U_i) from the behavior (B_i) is:

$$U_i(t) = P_i(t) \cdot u_i - C_i(t) \quad (9)$$

In this framework, an animal updates the probabilities for the different behaviors at each time step and selects the behavior that has the greatest expected utility.

The animal's probability estimate at time t depends on the probability at $t - 1$ and the new information available in the interval $t - 1$ to t . Expressing the proba-

Table 1
Numerical Fish Surrogate agents, behavior responses, and agent coefficients

i	Agent (A_i)	Behavior response (B_i)	u_i	m_i
0	Null	Follow flow	0.35	1.00
1	Wall-bounded flow gradient	Swim towards increasing water velocity	0.55	0.80
2	Free-shear flow gradient	Swim towards decreasing water velocity or against the flow vector	0.99	0.982
3	Pressure gradient	Swim toward acclimated depth	0.99	0.935

bility updating through an exponentially moving average gives:

$$P_i(t) = (1 - m_i) \cdot e_i(t) + m_i \cdot P_i(t - 1) \quad (10)$$

where $e_i(t)$ is a Boolean measure of the agent information in the time interval and m_i is a memory coefficient weighting the current information and the past probability $P_i(t - 1)$. Maintaining information across time steps produces movement exhibiting persistence, i.e., where direction of travel during time increment t to $t + 1$ depends on the increment $t - 1$ to t , which Wu et al. (2000) identify as an important feature in modeling animal movement.

In the Numerical Fish Surrogate, events identify whether or not the fish detects an agent. On detection the Boolean event measure is 1 and otherwise it is 0. Thus, for strain-based agent-behavior couplets, events are defined:

$$e_i(t) = \begin{cases} 0, & \text{if } \frac{I(t)}{I_a(t)} < k_i \\ 1, & \text{if } \frac{I(t)}{I_a(t)} \geq k_i \end{cases} \quad (11)$$

This definition of events is similar to Anderson’s (2002) definition in that they mark the presence or absence of an agent, and consistent with Workman et al. (2002, references therein) that threshold intensities can be cues that trigger fish movement.

Animals may perceive time according to the rate of events and not according to the fixed time increment convention typical of computer programming (Hills and Adler, 2002). In a time increment, if more than one event occurs for an agent, e.g., $I(t)/I_a(t) > 2k_1$, Eq. (10) may be applied recursively for the agent. This treatment has similarities to the definition of events used by Ewing et al. (2002), which denote a significant biological change resulting in an instantaneous state of change, and his event space concept where time is driven by the occurrence of events.

Information from the wall-bounded and free-shear flow gradients are not unique because both use strain information. Separating the information in terms of threshold levels, $k_2 > k_1$, is sufficient to differentiate between wall-bounded and free-shear flow gradient agents. However, stimuli variables may be refined as necessary. Indeterminacy is not a problem in the current formulation because the intrinsic utility of responding

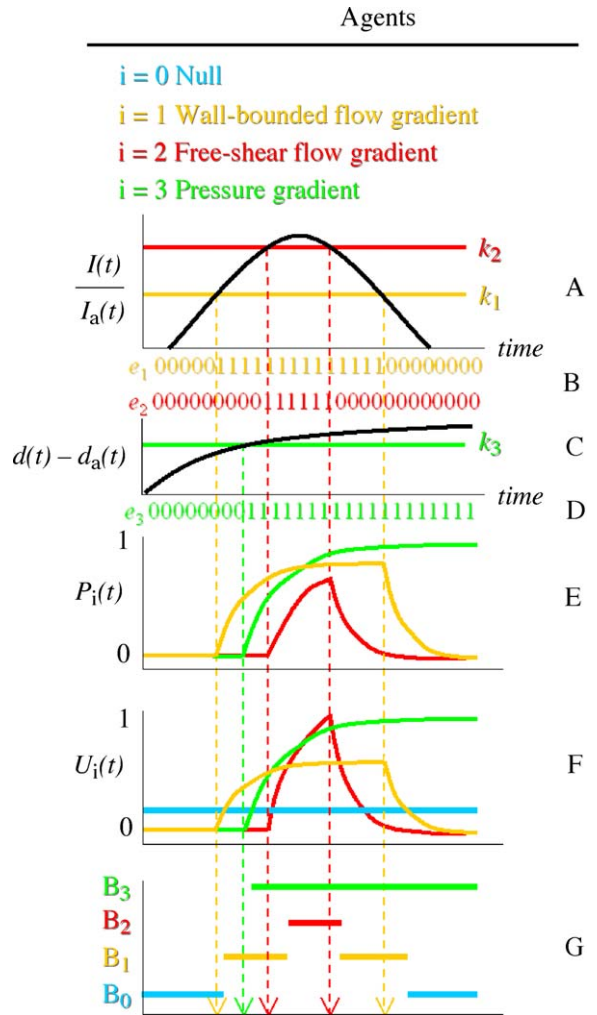


Fig. 7. Illustration of the agent-based, event-driven algorithm for migrants switching between behaviors B_0 , B_1 , B_2 , and B_3 . Time-varying changes in perceived strain relative to acclimated strain crossing thresholds k_1 and k_2 (A) produce Boolean event streams $e_1(t)$ and $e_2(t)$ (B) that generate time-varying probabilities $P(t)$ (E) and utilities $U(t)$ (F), where $u_2 > u_1$ and U_0 is time invariant. Changes in perceived pressure are handled analogously using a threshold k_3 (C) and event stream (D). Elicited behavior B_i (G) has the maximum expected utility $U(t)$ (F) at time t . When implemented, B_3 overrides other vertical movement behaviors.

to a free-shear flow gradient is greater than the intrinsic utility of responding to a wall-bounded flow gradient. The construct for the Numerical Fish Surrogate is illustrated in Fig. 7. Bioenergetic cost is not included in the present formulation.

3. Numerical Fish Surrogate application and evaluation

Hydropower dams on the Columbia and Snake Rivers (Fig. 2) contain a number of complex forebay structures to guide fish and trash away from turbines and past the dam. The Numerical Fish Surrogate is designed to be a decision-support tool that can (1) forecast observed (measured) trends in fish passage proportions and (2) rank fish bypass configurations by descending order of their measured passage proportions. The Numerical Fish Surrogate is calibrated with data for Lower Granite Dam forebay configuration DH8 (Fig. 1; Table 2). Data include: (1) high reso-

lution CFD model output to describe forebay hydrodynamic pattern, (2) horizontal and vertical distributions of migrants entering the dam forebay (Johnson and Kim, 2004), (3) detailed 3-D tracks of individual acoustically-tagged migrants (Cash et al., 2002), and (4) proportions of fish entering the spillway, turbines, and bypass (Surface Bypass Collector, Fig. 1) (Anglea et al., 2001). For validation, passage proportions forecast by the Numerical Fish Surrogate are compared to measured passage proportions at 19 other configurations: 2 at Ice Harbor Dam (Moursund et al., 2003), 5 at Wanapum Dam (LGL Limited, 2005), and 12 at Lower Granite Dam (Anglea et al., 2001, 2003; Plumb et al., 2004) (Table 2).

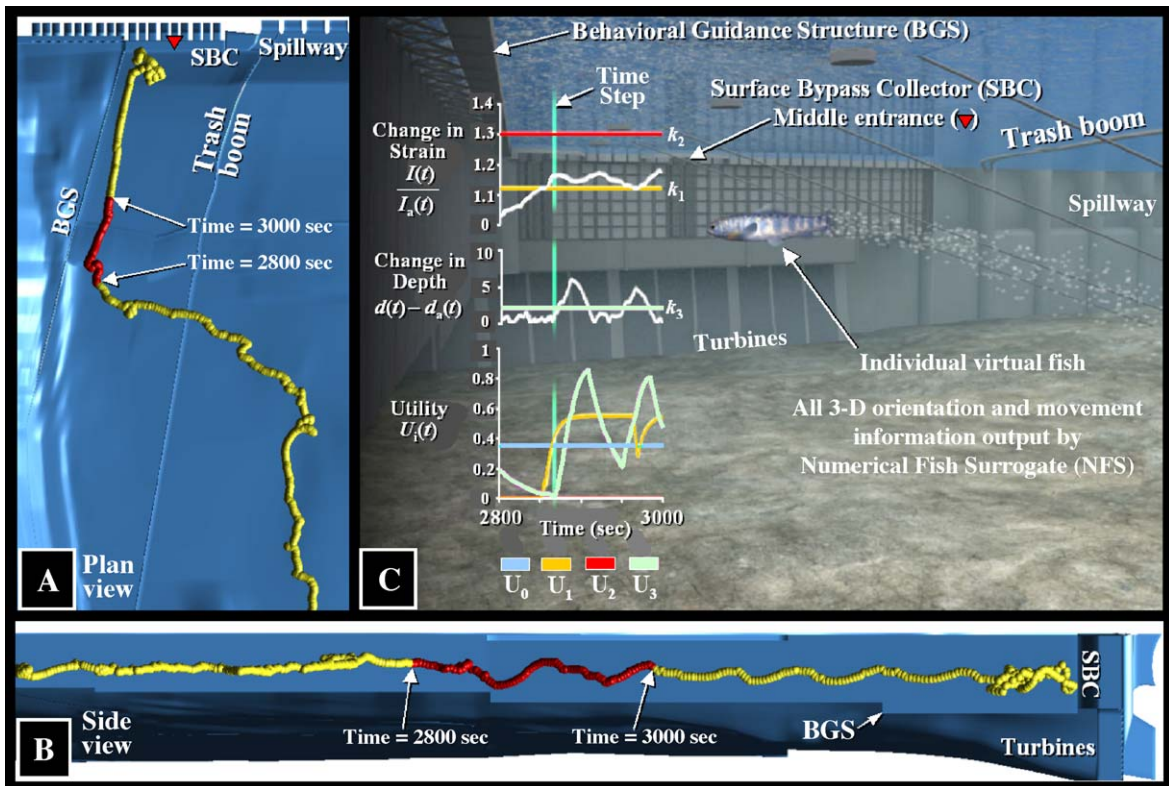


Fig. 8. Output from the Numerical Fish Surrogate showing the plan view (A) and vertical (B) movement of a virtual migrant responding to the Behavioral Guidance Structure (BGS, Fig. 1) for configuration DH8 (Table 2). Information streams of perceived changes in strain and depth and the resulting expected utility of each agent-behavior couplet (C) are displayed from time $t = 2800$ to 3000 s. This time interval corresponds to the highlighted (red) portion of the yellow virtual migrant 3-D track and is the time interval during which this virtual migrant first encounters the hydrodynamic pattern associated with the BGS. For reference, red triangle indicates location of middle entrance to SBC. Full video animation of fish movement behavior snapshot in (C) from time $t = 2800$ s to 3000 s can be downloaded from <http://EL.ercdc.usace.army.mil/emrrp/nfs/>.

Table 2
Dam structure and operational scenarios for Numerical Fish Surrogate studies

Passage route	Dam	Year	Case	Day/night	Passage (%)		CFD flow	
					Observed	NFS	m ³ /s	% of Total
(a) Bypass								
	IH	2003	BC1	Composite	0.0	0.0	0.0	0.0
		2003	BC3	Composite	0.0	0.0	0.0	0.0
	WAN	1997	1997_AFP	Composite	3.0	3.1	101.9	1.4
		2001	2001	Composite	40.2	31.3	48.1	2.6
		2002	2002_Mixed	Composite	26.7	24.6	337.0	8.4
		2002	2002_MOA	Composite	6.9	7.5	53.8	1.3
		2002	2002_TopSpill	Composite	17.9	15.5	345.5	8.3
	LG	2003	AR6	Composite	68.0	59.3	198.2	10.9
		2003	NR3	Composite	59.0	50.3	198.2	9.3
		2000	DH8	Composite	36.0	25.7	99.1	3.8
		2000	DL5	Composite	37.0	32.5	99.1	5.1
		2000	SH4	Composite	44.0	51.0	99.1	4.3
		2000	SL2	Composite	42.0	53.2	99.1	4.1
		2002	A2	Composite	78.0	44.6	198.2	9.3
		2002	B2	Composite	73.9	63.5	198.2	10.4
		2002	C2	Day	1.5	0.0	0.0	0.0
		2002	D2	Night	2.0	0.0	0.0	0.0
		2002	E2	Composite	41.7	48.2	198.2	6.0
		2002	F2	Day	0.4	0.0	0.0	0.0
		2002	G2	Night	0.0	0.0	0.0	0.0
		(b) Spillway						
	IH	2003	BC1	Composite	78.5	78.1	1265.8	59.8
		2003	BC3	Composite	89.5	79.1	1246.0	58.6
	WAN	1997	1997_AFP	Composite	61.0	45.2	2829.0	39.2
		2001	2001	Composite	24.5	5.7	611.7	32.7
		2002	2002_Mixed	Composite	14.7	9.6	640.0	16.0
		2002	2002_MOA	Composite	33.7	35.9	1485.6	35.9
		2002	2002_TopSpill	Composite	0.0	0.0	0.0	0.0
	LG	2003	AR6	Composite	5.0	10.0	339.8	18.8
		2003	NR3	Composite	6.0	8.9	240.7	11.3
		2000	DH8	Composite	24.0	23.3	450.3	17.3
		2000	DL5	Composite	23.0	24.5	351.1	18.0
		2000	SH4	Composite	22.0	22.2	450.3	19.5
		2000	SL2	Composite	22.0	22.8	450.3	18.7
		2002	A2	Composite	3.1	10.2	240.7	11.3
		2002	B2	Composite	9.5	23.4	438.9	23.0
		2002	C2	Day	2.2	0.0	0.0	0.0
		2002	D2	Night	89.3	76.8	1223.3	45.9
		2002	E2	Composite	47.7	42.7	1427.2	43.3
		2002	F2	Day	69.5	36.8	693.8	26.2
		2002	G2	Night	87.6	73.2	1483.9	49.2
		(c) Turbines						
	IH	2003	BC1	Composite	21.5	21.9	849.5	40.2
		2003	BC3	Composite	10.5	20.9	880.7	41.4

Table 2 (Continued)

Passage route	Dam	Year	Case	Day/night	Passage (%)		CFD flow	
					Observed	NFS	m ³ /s	% of Total
	WAN	1997	1997_AFP	Composite	36.0	51.7	4281.7	59.4
		2001	2001	Composite	32.3	63.0	1212.0	64.8
		2002	2002_Mixed	Composite	56.6	65.8	3032.8	75.6
		2002	2002_MOA	Composite	58.4	56.6	2603.5	62.8
		2002	2002_TopSpill	Composite	91.1	84.5	3811.6	91.7
	LG	2003	AR6	Composite	27.0	30.7	1274.3	70.3
		2003	NR3	Composite	34.0	40.8	1699.1	79.5
		2000	DH8	Composite	40.0	51.0	2055.9	78.9
		2000	DL5	Composite	40.0	42.9	1498.0	76.9
		2000	SH4	Composite	34.0	26.8	1755.7	76.2
		2000	SL2	Composite	36.0	24.1	1860.5	77.2
		2002	A2	Composite	18.9	45.1	1699.1	79.5
		2002	B2	Composite	16.7	13.2	1274.3	66.7
		2002	C2	Day	96.3	100.0	1812.3	100.0
		2002	D2	Night	8.7	23.2	1444.2	54.1
		2002	E2	Composite	10.5	9.1	1670.8	50.7
		2002	F2	Day	30.1	63.2	1953.9	73.8
		2002	G2	Night	12.4	26.8	1529.2	50.8

IH, Ice Harbor Dam on Snake River; observed hydroacoustic based passage % from Moursund et al. (2003). WAN, Wanapum Dam on Columbia River; observed radio-tag based passage % from LGL Limited (2005). LG, Lower Granite Dam on Snake River; observed hydroacoustic based passage % in 2000 and 2002 from Anglea et al. (2001, 2003) and radio-tag based passage % in 2003 from Plumb et al. (2004). Numerical Fish Surrogate (NFS) passage % based on 5000 virtual migrants.

3.1. Calibration

Calibration is a two-phase process. First, model coefficients k_i , m_{strain} , m_{depth} , m_i , and u_i are adjusted until individual virtual migrant tracks calculated at 2.0-s time increments qualitatively resemble movement patterns of acoustically-tagged migrants for configuration DH8 (Fig. 1; Table 2). Next, coefficients are fine-tuned so that the passage proportions of 2000 virtual migrants released upstream quantitatively resemble the measured passage proportions through the bypass (Table 2a), spillway (Table 2b), and turbines (Table 2c) for configuration DH8.

3.1.1. Matching movement patterns of real and virtual migrants

To illustrate the first phase of calibration, we detail the interactions of a virtual migrant (Fig. 8) with its hydrodynamic environment (Fig. 9) as it approaches and then parallels the Behavioral Guidance Structure (BGS, Fig. 1) over a 200-s interval. At the beginning of the interval ($t=2800$ s) the changes in perceived strain and depth are small, utility U_0 dominates, and the virtual migrant elicits behavior B_0 (Table 1). The change

in perceived strain increases as the virtual migrant approaches elevated strain associated with the BGS (Fig. 9, right plots) and at $t=2850$ s exceeds threshold k_1 . Utility U_1 exceeds U_0 at $t=2860$ s and the virtual migrant switches from behavior U_0 to U_1 . The migrant also encounters increasing downward velocity associated with flow passing under the BGS (Fig. 10) increasing the change in perceived pressure. At $t=2875$ s, utility U_3 exceeds U_1 eliciting vertical behavior B_3 that overrides the vertical behavior component of U_1 until $t=2925$ s when U_3 drops below U_1 . Acclimated strain $I_a(t)$ and depth $d_a(t)$ adjust to new levels each time step and the behavior cycle repeats as the virtual migrant moves along the BGS. Both acoustically-tagged (Fig. 11) and virtual (Fig. 8) migrants deeper in the water column pass under the trash boom with no apparent response (Figs. 8A and 11B), approach the BGS at approximately the same angle as flow (Figs. 8A, 10, and 11B), move parallel to the BGS in a vertically oscillatory manner (Figs. 8B and 11), and mill below the entrance to the SBC closest to the BGS and above the turbine intakes (Figs. 8A and B and 11A). Acoustically-tagged migrants in Fig. 11 were observed at night so visual cues are not likely dominant.

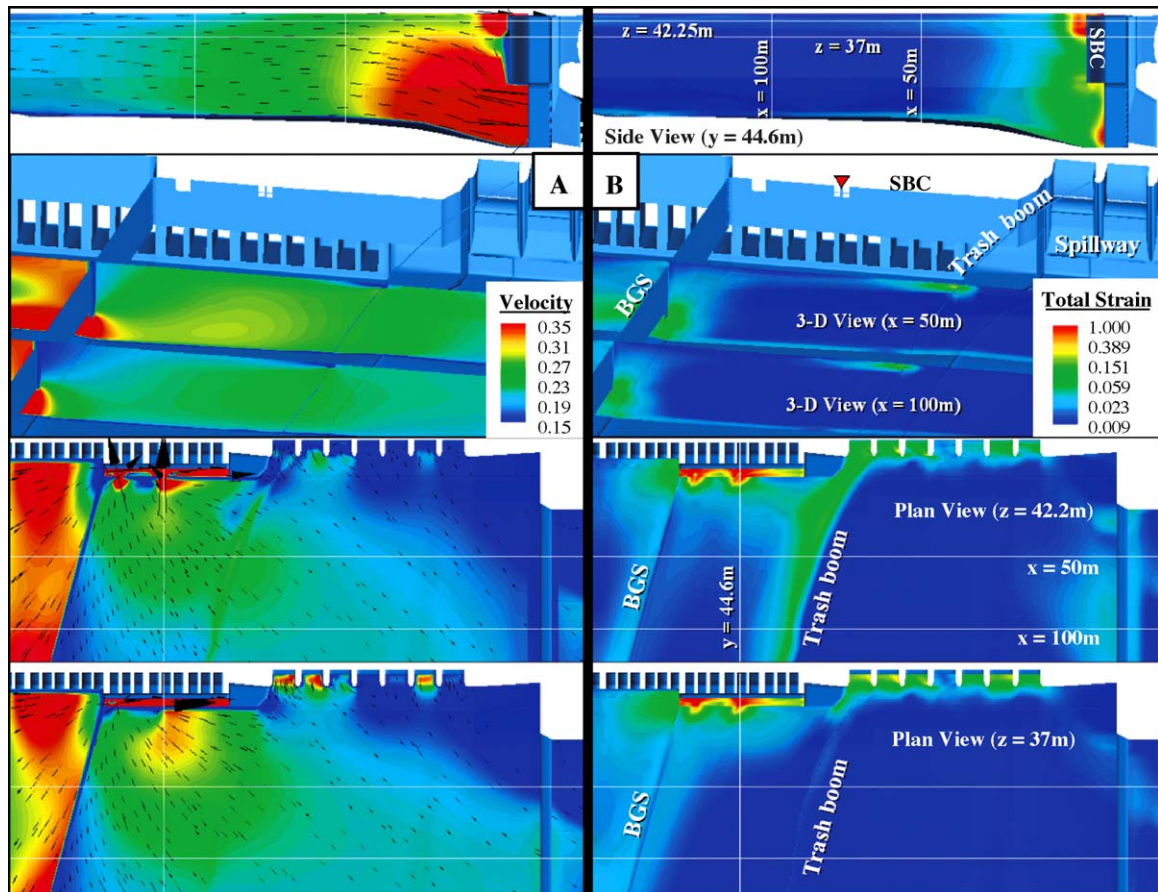


Fig. 9. Velocity magnitude (A, plots on left) and hydraulic strain (B, plots on right) for configuration DH8 (Table 2). Cross-sectional slices taken through middle entrance to the SBC ($y = 44.6$ m), cross-sectional slices parallel to dam face ($x = 50$ and 100 m), and plan view slices ($z = 37$ and 42.25 m) show the change in hydrodynamic pattern at different locations and depths. Water surface elevation is 44.7 m.

Migrants nearer the water surface exhibit different movement patterns also matched by the Numerical Fish Surrogate. Both acoustically-tagged (Fig. 12B and C) and virtual (Fig. 12A) migrants near the water surface move back and forth between the middle SBC entrance (Fig. 1) and the powerhouse side of the trash boom, but avoid areas near the BGS. Both acoustically-tagged and virtual migrant movement patterns are in sharp contrast to movement patterns of passive particles (Fig. 12D). The apparent difference in acoustically-tagged migrant movement patterns at near-surface (Fig. 12B and C) and deeper (Fig. 11) depths are matched by virtual migrants whose behavior is attributable to the different hydrodynamic patterns encountered at different depths (Fig. 9).

Lastly, acoustically-tagged and virtual migrants have similar modes and right-skewed frequency distributions of swimming speed (Fig. 13). Discrepancies in sampling intervals between acoustically-tagged and virtual migrants and the correlation between spatial location and frequencies of acoustically-tagged migrant observations preclude a more quantitative comparison.

3.1.2. Matching patterns in fish passage proportion

After the Numerical Fish Surrogate approximates the predominant movement patterns of individual acoustically-tagged migrants, agent coefficients are fine-tuned until the passage proportions of 2000 virtual

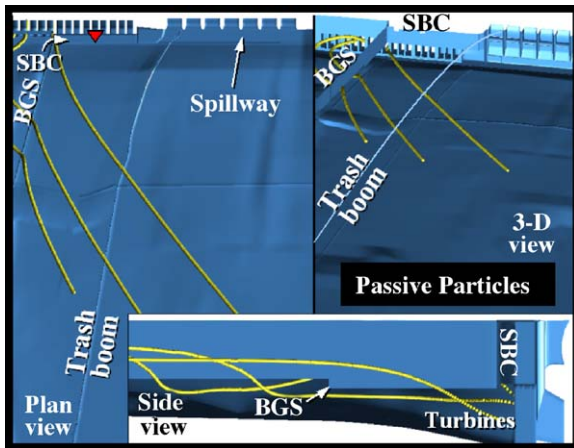


Fig. 10. Three neutrally-buoyant passive particles (behavior rules turned OFF) released at approximately the same depths as virtual migrant in Fig. 8 and acoustically-tagged migrants in Fig. 11 for configuration DH8 (Table 2).

migrants resemble the observed (measured) passage proportions from fixed-location hydroacoustic instrumentation for configuration DH8 (Anglea et al., 2001). Our goal is to match the observed proportions from hydroacoustic and radio-tag measurement techniques within about $\pm 10\%$.

Two thousand virtual migrants are released in the middle 80% of the river cross-section to avoid corrupting $I_a(t)$ with localized boundary-induced hydraulics. Virtual migrants are also released about a kilometer upstream from the dam to allow time for $I_a(t)$ and $d_a(t)$ to stabilize, prior to encountering the high-energy hydrodynamic patterns of the dam (Fig. 9). Upstream day and night vertical distributions of migrants are obtained from published reports covering a variety of methods (Johnson and Kim, 2004) to capture observed diel changes close to dams (Steig and Johnson, 1986; Coutant and Whitney, 2000; Cash et al., 2002) (Fig. 14). A composite of day and night vertical distributions is used for configurations not categorized as either day- or night-only studies (Table 2).

3.2. Validation

The calibrated Numerical Fish Surrogate is validated against 19 different structural and operational bypass configurations at 3 hydropower dams on 2

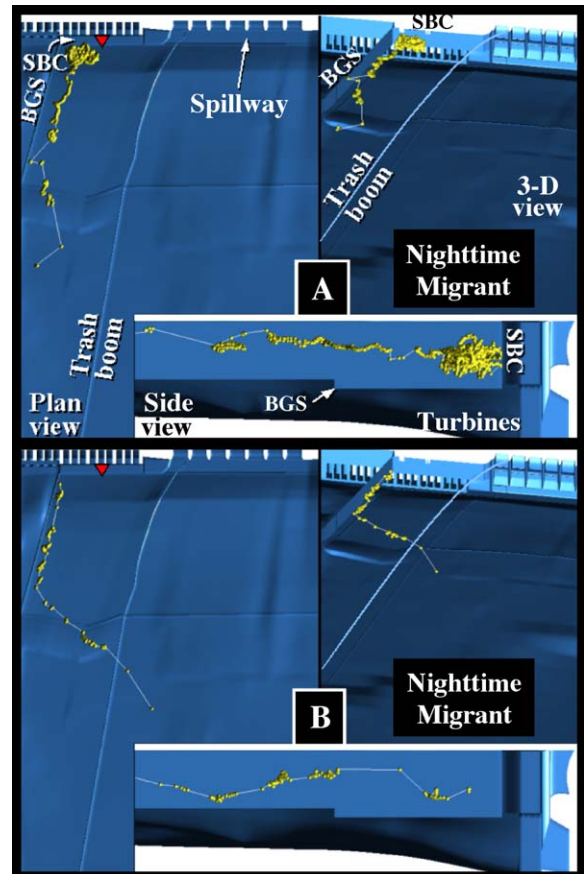


Fig. 11. Representative acoustically-tagged migrant movement patterns at depths similar to virtual migrant in Fig. 8 and passive particles in Fig. 10 for configuration DH8 (Table 2). Acoustic-tag data from Cash et al. (2002).

ivers (Fig. 2; Table 2). Improvements in the memory allocation of the Numerical Fish Surrogate permitted simulation of 5000 virtual migrants at this stage in the study. Forecasted passage proportions for the calibration configuration DH8 did not change substantially with the increase from 2000 to 5000 virtual migrants.

We use two metrics to assess the forecasting capability of the Numerical Fish Surrogate: (1) ability to forecast measured trends in fish passage proportions using a linear regression of measured versus forecasted values (Smith and Rose, 1995) and (2) ability to rank configurations by descending order of their measured passage proportions. Observations and forecasts at bypass,

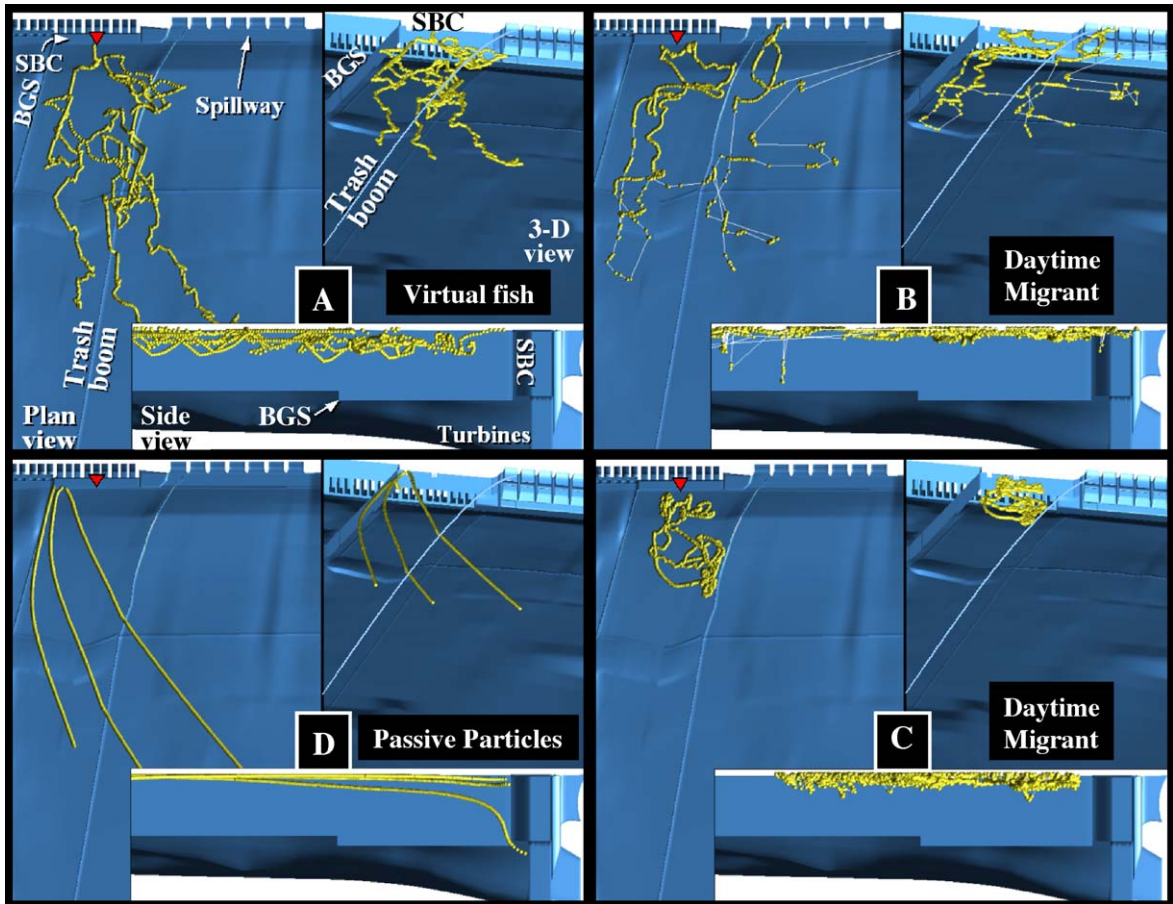


Fig. 12. Comparison of representative near-surface virtual (A) and acoustically-tagged (B and C) migrant movement patterns for configuration DH8 (Table 2). Three neutrally-buoyant passive particles (behavior rules turned OFF) (D) released near water surface at same locations as virtual migrants in (A). Acoustic-tag data from Cash et al. (2002).

spillway, and turbine passage routes with either 0% or 100% of the river flow in the CFD model (Table 2) are not used in the analysis. The results of the Numerical Fish Surrogate generally match measured trends in passage for the three possible exit routes (Fig. 15A; Table 3). Concurrence between observed (measured) and virtual distributions is a strong test of a model (Bart, 1995) especially when r^2 exceeds 0.65 (Prairie, 1996). The passage of passive particles (“behavior rules off”) released at the virtual migrant locations differed substantially from either measured passage or “behavior rules on” forecasts (Fig. 15B; Table 3). The Numerical Fish Surrogate also generally matches the observed ranking of configurations as top-, moderate-, and low-

performing using the metric of passage per unit of modeled flow for bypass (Table 4a), spillway (Table 4b), and turbines (Table 4c). The larger variability between measured and forecasted turbine passage proportions (Fig. 15A; r^2 in Table 3) is likely related to the larger variability of powerhouse operations. Even when total powerhouse discharge is held constant during a field study, turbine units in operation and the distribution of load across those units typically changes with much greater variability than observed with either spillway or bypass operations. Thus, the steady-state CFD model we use better captures the hydrodynamic stimulus patterns at spillway and bypass passage routes than at the powerhouse.

Table 3
Slopes of and variation (r^2) about linear regression trend lines in Fig. 15

Release distribution	Passage route	Behavior rules	Slope	r^2
Calibration/validation	Bypass	ON	0.74	0.78
		OFF	0.17	0.39
	Spillway	ON	0.77	0.89
		OFF	0.49	0.54
	Turbines	ON	0.82	0.65
		OFF	0.32	0.14
Sensitivity analysis	Bypass	ON	1.07	0.80
		OFF	0.10	0.10
	Spillway	ON	0.95	0.85
		OFF	0.49	0.50
	Turbines	ON	1.15	0.61
		OFF	0.24	0.08

Calibration/validation release distribution (Fig. 14) from Johnson and Kim (2004). Sensitivity analysis release distribution (Fig. 14) from Faber et al. (2004).

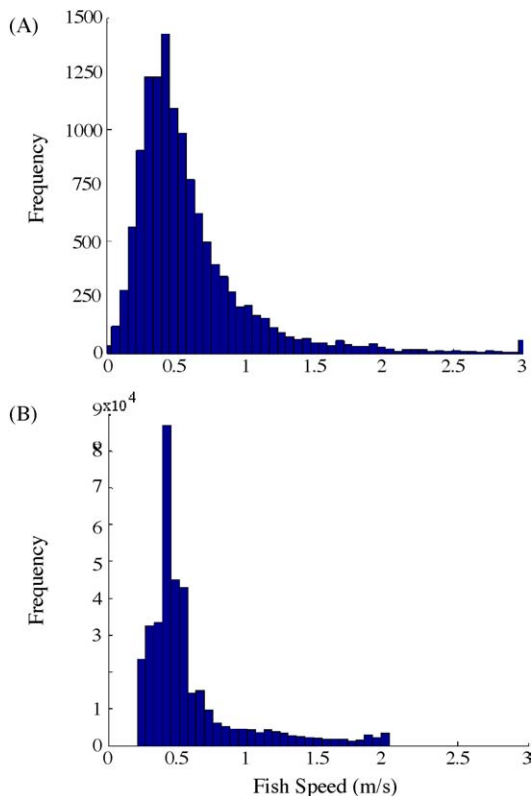


Fig. 13. Volitional swim speed distributions of nighttime acoustically-tagged (A) and 100 virtual (B) migrants for configuration DH8 (Table 2). Acoustic-tag data filtered to exclude observations where tagged migrants may have exited and re-entered the observation area. Acoustic-tag data from Cash et al. (2002).

3.3. Sensitivity analysis

We perform a basic sensitivity analysis of the Numerical Fish Surrogate to gauge the resilience of forecasted passage results when biological input is changed. We use a depth distribution of migrants observed upstream of The Dalles Dam on the Columbia River (Fig. 14; Faber et al., 2004) to determine sensitivity of the Numerical Fish Surrogate to initial release distribution. Slopes and r^2 s for the “behavior rules on” sensitivity release distribution indicate the Numerical Fish Surrogate generally matches the measured passage proportions as well as the calibration/validation release distribution (Fig. 15A–C; Table 3). Slopes and r^2 s for the “behavior rules off” sensitivity release distribution are slightly worse than for the calibration/validation release distribution (Fig. 15B–D; Table 3).

4. Discussion

4.1. The Numerical Fish Surrogate

The Numerical Fish Surrogate forecasts reasonably well the response of individual migrants to specific hydraulic features and generally forecasts group response of large numbers of migrants to alternative bypass system designs. These capabilities suggest the

Table 4
Ranking of configurations by observed and forecasted passage metrics

Passage route	Case	Passage (% per unit flow)					
		Observed	Observed rank	NFS (rules ON)	NFS rank (rules ON)	NFS (rules OFF)	NFS rank (rules OFF)
(a) Bypass							
	2001	0.835	1	0.604	1	0.037	11
	SH4	0.444	2	0.512	3	0.059	7
	SL2	0.424	3	0.535	2	0.062	6
	A2	0.393	4	0.225	10	0.075	3
	DL5	0.373	5	0.328	4	0.067	4
	B2	0.373	6	0.319	5	0.064	5
	DH8	0.363	7	0.258	7	0.049	8
	AR6	0.343	8	0.299	6	0.098	1
	NR3	0.298	9	0.253	8	0.079	2
	E2	0.211	10	0.239	9	0.043	10
	2002_MOA	0.128	11	0.125	11	0.013	13
	2002_Mixed	0.079	12	0.068	12	0.034	12
	2002_TopSpill	0.052	13	0.041	13	0.043	9
	1997_AFP	0.029	14	0.028	14	0.005	14
	BC1	–	–	–	–	–	–
	BC3	–	–	–	–	–	–
	C2	–	–	–	–	–	–
	D2	–	–	–	–	–	–
	F2	–	–	–	–	–	–
	G2	–	–	–	–	–	–
(b) Spillway							
	F2	0.100	1	0.053	6	0.038	13
	D2	0.073	2	0.063	2	0.034	14
	BC3	0.072	3	0.061	3	0.057	2
	DL5	0.066	4	0.070	1	0.057	4
	BC1	0.062	5	0.060	4	0.057	3
	G2	0.059	6	0.049	9	0.030	16
	DH8	0.053	7	0.052	7	0.042	10
	SL2	0.049	8	0.050	8	0.046	7
	SH4	0.049	9	0.049	10	0.044	8
	2001	0.040	10	0.009	18	0.069	1
	E2	0.033	11	0.029	13	0.028	17
	NR3	0.025	12	0.037	12	0.044	9
	2002_Mixed	0.023	13	0.014	17	0.042	11
	2002_MOA	0.023	14	0.021	15	0.031	15
	1997_AFP	0.022	15	0.015	16	0.017	18
	B2	0.022	16	0.053	5	0.056	5
	AR6	0.015	17	0.029	14	0.039	12
	A2	0.013	18	0.042	11	0.049	6
	2002_TopSpill	–	–	–	–	–	–
	C2	–	–	–	–	–	–
(c) Turbines							
	C2	0.053	1	0.055	1	0.055	1
	DL5	0.027	2	0.029	4	0.049	4
	2001	0.027	3	0.048	2	0.033	13
	BC1	0.025	4	0.025	6	0.027	15
	2002_TopSpill	0.024	5	0.020	11	0.020	17
	2002_MOA	0.022	6	0.019	13	0.014	19
	AR6	0.021	7	0.024	8	0.053	2

Table 4 (Continued)

Passage route	Case	Passage (% per unit flow)					
		Observed	Observed rank	NFS (rules ON)	NFS rank (rules ON)	NFS (rules OFF)	NFS rank (rules OFF)
	NR3	0.020	8	0.024	9	0.043	5
	DH8	0.019	9	0.025	7	0.037	11
	SH4	0.019	10	0.015	16	0.042	7
	SL2	0.019	11	0.013	17	0.040	9
	2002_Mixed	0.019	12	0.020	12	0.018	18
	F2	0.015	13	0.032	3	0.038	10
	B2	0.013	14	0.010	19	0.049	3
	BC3	0.012	15	0.023	10	0.027	16
	A2	0.011	16	0.027	5	0.043	6
	1997_AFP	0.008	17	0.011	18	0.008	20
	G2	0.008	18	0.017	14	0.036	12
	E2	0.006	19	0.005	20	0.031	14
	D2	0.006	20	0.016	15	0.041	8

Numerical Fish Surrogate and embodied SVP Hypothesis provide a sufficient understanding of migrant passage dynamics to identify opportunities for cost-effective intervention to improve system operation (Stedinger, 2000). As a tool, the Numerical Fish Surrogate can be integrated into common engineering prac-

tice where fish behavior is an important element of water resources planning in a manner suggested by Popper and Carlson (1998).

Our application documents response of migrants to hydrodynamic patterns in dam forebays. However, the Numerical Fish Surrogate may also be applied to

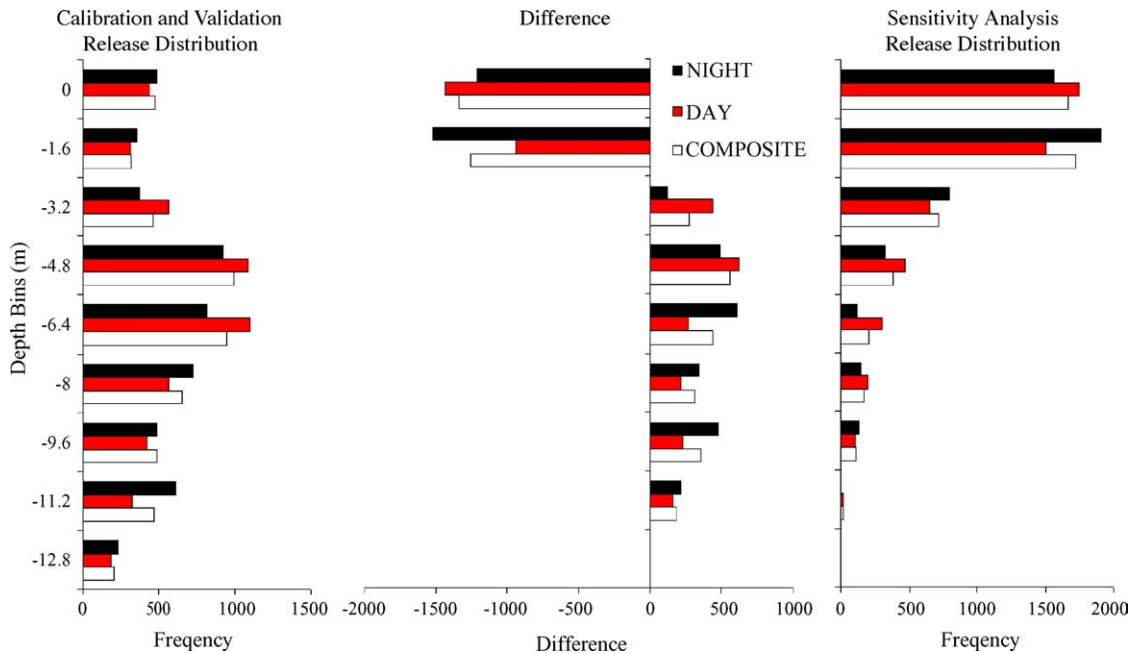


Fig. 14. Depth distributions of 5000 virtual migrants released at Lower Granite Dam for calibration and validation (Johnson and Kim, 2004) and for sensitivity analysis (Faber et al., 2004).

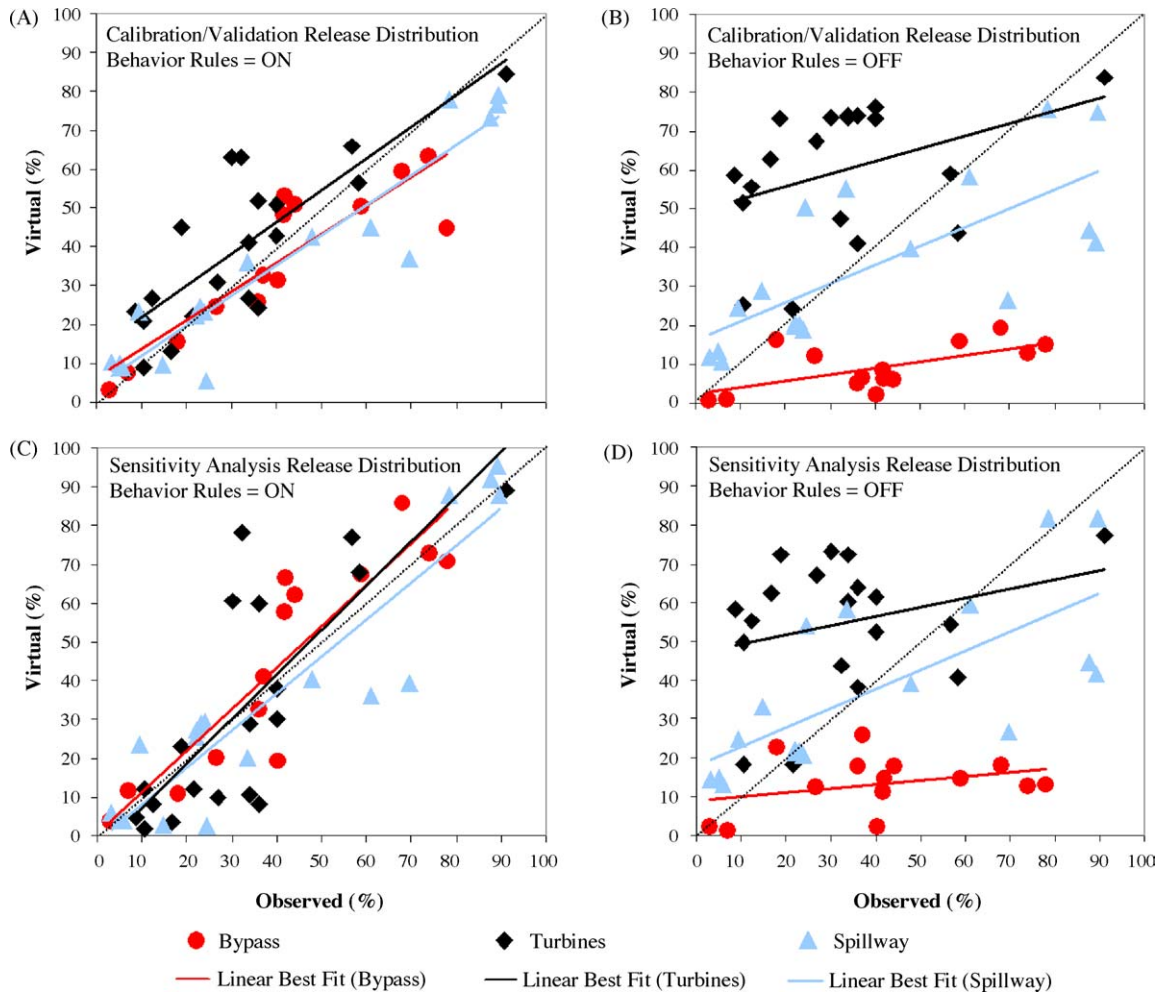


Fig. 15. Comparison of observed (measured) and Numerical Fish Surrogate (NFS) virtual migrant passage proportions, on a percentage basis, for configurations in Table 2 using calibration/validation release distribution (Fig. 14) (A). Comparison of observed and passive particle passage proportions, on a percentage basis, using calibration/validation release distribution (B). Comparison of observed and virtual migrant passage proportions, on a percentage basis, using sensitivity analysis release distribution (Fig. 14) (C). Comparison of observed and passive particle passage proportions, on a percentage basis, using sensitivity analysis release distribution (D). NFS virtual passage proportions based on 5000 virtual migrants. Passage (exit) routes are bypass, spillway, and turbines. Slopes of and variation about each of the linear regression trend lines summarized in Table 3. Routes with either 0% or 100% of river flow in CFD model are not plotted or factored into trend lines. Observed (measured) Lower Granite Dam hydroacoustic based migrant passage proportions in 2000 and 2002 from Anglea et al. (2001, 2003), radio-tag based migrant passage proportions in 2003 from Plumb et al. (2004), Ice Harbor Dam hydroacoustic based migrant passage proportions from Moursund et al. (2003), and Wanapum Dam radio-tag based migrant passage proportions from LGL Limited (2005).

tailraces where migrants can be subjected to injury and mortality in the high-energy hydraulic environments (Coutant, 1987; Christie and Regier, 1988). The Numerical Fish Surrogate can be used to improve the assessment of how different structural and operational alternatives impact the volitional egress move-

ments, predator locations and predator-prey interactions (Petersen and DeAngelis, 2000; Anderson et al., 2005), and temperature and dissolved gas exposure histories (Anderson, 2000a; Backman et al., 2002; Nestler et al., 2002; Scheibe and Richmond, 2002) of fish in tailraces.

4.1.1. Archiving knowledge for fish passage

Presently, fish passage design relies on a “build-and-test paradigm” to select from among alternative competing structures. Over a period of time, the selected alternative is monitored, evaluated, and incrementally improved until a target passage is obtained. However, the “build-and-test paradigm” is expensive, inefficient, and impacts fish populations as scientists and engineers incrementally improve bypass performance, often with little or no scientific advancements in understanding fish behavior. The Numerical Fish Surrogate is a theoretically- and computationally-robust method to integrate, better understand, and forecast fish movement in hydrodynamic and water quality fields as first advocated by Anderson (1988). It can reduce reliance on the “build-and-test paradigm”. Fish movement response to patterns in available biotic and abiotic stimuli are decoded into a mechanistic biological hypothesis of individual fish behavior using agents and coefficients for a given target species and life-stage. The Numerical Fish Surrogate then serves as a knowledge base for qualitative and quantitative understanding of fish movement behavior as the equations describing a particular hypothesis about fish movement and passage behaviors are updated and improved. These updates may quantitatively capture and describe how passage behavior changes by species, race, size, or other variables. This knowledge can be ported to other locales where designs for passage of the same species and life-stage are needed.

4.2. The Eulerian–Lagrangian–agent method

The Eulerian–Lagrangian–agent method (ELAM) used for the Numerical Fish Surrogate can be considered from a broad philosophical perspective, or from a specific application. From a philosophical perspective, methods to explore, formalize, and forecast dynamics of complex, multi-scale processes, typical of ecosystem dynamics, can be categorized as Eulerian, Lagrangian, or agent. We know of no other frameworks for handling the spatial dynamics of animal movement (Parrish and Edelstein-Keshet, 1999). Coupled Eulerian–Lagrangian–agent frameworks, although mathematically and computationally challenging, can be used to address a wide variety of simulation challenges because the coupling architecture allows each frame to be applied at the scale

for which it is best suited. ELAM modeling systems like the Numerical Fish Surrogate can be considered to be a single, integrated knowledge engine in which information can be rotated, translated, converted, or rescaled, as needed, to be used by any one of the three frameworks. In such an integrated system, the Eulerian framework efficiently simulates processes in which the entity of interest is small relative to the physical domain of the study system. The entities can be aggregated into control volumes and their dynamics simplified as cell masses and fluxes without significant errors of aggregation. This simplification comes at the loss of identity during aggregation (Nestler et al., 2005). The Lagrangian framework efficiently simulates entities intermediate in size relative to the physical domain of the system or have other attributes that result in unacceptable accumulation of error during aggregation. The Lagrangian frame allows the integrity and separate identity of each individual to be maintained and tracked within an analysis, but often at the expense of computational time. The agent framework is well suited for entities requiring governing equations separate from the rest of the system, either because of their large relative size or because of unique behavior. Within the Numerical Fish Surrogate, the CFD model represents the Eulerian frame, particles and particle traces represent the Lagrangian frame, and behavioral rules represent the agent frame.

At an application level perspective, ELAM models like the Numerical Fish Surrogate address several needs in ecological modeling: (1) conversion of information from sources that differ in metric, range, scale, and dimensionality to a form of computer script (agents) that corresponds to animal perceptions (Bian, 2003), (2) ability to systematically organize and evaluate behavior hierarchies from the integration of information from various sensory modalities that may take varying precedence during the changing phases of a behavioral sequence (Sogard and Olla, 1993; New et al., 2001), (3) decentralized computer script for adding, eliminating, or modifying components without affecting the rest of the model (Ginot et al., 2002), (4) the theoretical and computational basis to elicit vector-based movement of individuals responding to abiotic and biotic stimulus data provided in either Eulerian (Tischendorf, 1997) or Lagrangian forms (Nestler et al., 2005), and (5) ability to easily compare model results to field-collected data (Hastings and Palmer, 2003). Vir-

tual individuals can then be used to explore plausible movement strategies of real individuals. Each virtual individual may represent an individual or some aggregate of the real population having attributes of species, size, age, life-stage, or other attributes necessary for realistic simulation. Virtual sampling (Halle and Halle, 1999; Goodwin et al., 2001; Nestler et al., 2005) that considers limitations and biases of the field sampling protocol can then be used with statistics to assess model performance (Grimm et al., 1999).

The Eulerian–Lagrangian-agent method (ELAM) in this paper derives from the integration of methods in Goodwin et al. (2001) and Anderson (2002), but embodies many features of the following methods: Eulerian–Lagrangian methods (ELMs) used in the study and simulation of hydrodynamics (Costa and Ferreira, 2000), coupled modeling (DeAngelis and Cushman, 1990; Hanna et al., 1999; Nestler et al., 2005), grid-, agent-, and object-oriented concepts for describing the environment (Lai et al., 2003a; Bian, 2003), event-based concepts (Ewing et al., 2002), spatially-explicit IBMs (Dunning et al., 1995; Romey, 1996; Clark and Rose, 1997; Van Winkle et al., 1998; Railsback et al., 1999a; Dagorn et al., 2000; Gaff et al., 2000; Petersen and DeAngelis, 2000; Xiao, 2000), linked models of environmental dynamics and individual fish behavior (Hinckley et al., 1996; Bourque et al., 1999; Railsback et al., 1999b; Anderson, 2000b; Haefner and Bowen, 2002; Hinrichsen et al., 2002; Nestler et al., 2002; Karim et al., 2003), and particle-based simulations (Haefner and Bowen, 2002; Scheibe and Richmond, 2002).

4.3. Future directions

4.3.1. Emerging modeling technologies

Mismatch between spatial scales at which hydraulics are modeled and scales at which fish respond affects accuracy of fish behavior simulation (Kondolf et al., 2000; Bult et al., 1999; Railsback, 1999). Flow may become unsteady and hydraulic gradients become more pronounced in the high-energy environment close to the openings of fish passage facilities. In such settings, steady-state RANS CFD modeling may be inadequate and improved CFD modeling methods may be needed to accurately decode and forecast fish movement. We believe new, emerging methods such as large-eddy simulation

(LES) CFD modeling (e.g., Mahesh et al., 2004; McCoy et al., 2005; Tokyay and Constantinescu, 2005) may be needed to more accurately resolve eddy formation and turbulence production at spatiotemporal scales important to fish behavior.

4.3.2. Expanding accuracy and usefulness of ELAM models

Accuracy and usefulness of ELAMs can be improved and expanded, respectively. To improve accuracy, genetic algorithm optimization methods can be employed to efficiently calibrate coefficients with suitable optimization metrics. Calibration methods tailored for models with synergies (e.g., van Nes et al., 2002) can also be employed. Ecological modeling may be enhanced through employment of an ELAM framework to integrate algorithms of movement behavior, bioenergetics and foraging (e.g., Stockwell and Johnson, 1997), growth, recruitment, mortality, nutrient cycling (e.g., Schindler and Eby, 1997), and schooling and/or predator–prey interactions (e.g., Huth and Wissel, 1992, 1994; Niwa, 1994; Nonacs et al., 1994; Reuter and Breckling, 1994).

Embedding existing algorithms of population dynamics into an ELAM model provides a well suited construct for studying and modeling the exposure histories of individuals to environmental conditions (e.g., Smith et al., 2002), overlap dynamics with other species (e.g., Pientka and Parrish, 2002), and interspecific competition and predation (e.g., Reese and Harvey, 2002). ELAM models coupled with water quality and eutrophication models provide a framework from which to improve existing efforts (e.g., Karim et al., 2003) to understand and forecast the impact of changes in land use on the movement and health of aquatic species. ELAMs can also simulate the inverse problem where highly mobile species may be a factor in the movement of a contaminant as described in Monte (2002).

In summary, Eulerian–Lagrangian–agent methods (ELAMs) provide a robust theoretical and computational foundation to mathematically interpret the movement of individuals useful for forecasting population patterns. ELAMs can accommodate algorithms from the field of individual-based modeling to formulate a modeling framework with an expanded ecosystem perspective for system-wide analyses. Optimization and simulation methods frequently used in water

resource systems engineering (e.g., Loucks et al., 1981; Loucks and van Beek, 2005) can then be used to develop improved management strategies (e.g., Jager and Rose, 2003) using transparent and intuitive means that are also easy to visualize, communicate, and evaluate.

Acknowledgements

The tests described and the resulting data presented herein, unless otherwise noted, were obtained from research conducted under the sponsorship of the U.S. Army Engineer District Walla Walla, the Grant County Public Utility District, and the System-Wide Water Resources Program (SWWRP), a U.S. Army Corps of Engineers research and development initiative. We gratefully acknowledge Lynn Reese and Mark Lindgren of Walla Walla District for funding support, Songheng Li of the University of Iowa—IIHR and Yong Lai (now with U.S. Bureau of Reclamation) for providing CFD model simulation data and cooperation, Ken Cash of the U.S. Geological Survey for collecting and filtering the acoustic-tag data, Gary Johnson and Kenneth Ham of Battelle Pacific Northwest National Lab for collecting and filtering hydroacoustic passage data, Carl Schilt and Jina Kim of BAE Systems, Inc. for help with sensory biology concepts and post-processing, respectively, Ray Chapman of the U.S. Army Engineer Research and Development Center (ERDC) and Terry Gerald of ASCI for help with contravariant mathematics, and Toni Toney and Dottie Tillman of ERDC for modeling support. Software and software license information can be obtained from the Office of Research Technology, ERDC (Telephone: +1 601 634 4113). 3-D computer virtual fish animations and further information on Eulerian–Lagrangian–agent methods (ELAMs) can be found at <http://EL.ercd.usace.army.mil/emrrp/nfs/>. Permission was granted by the Chief of Engineers to publish this information.

References

- Anderson, J.J., Gurarie, E., Zabel, R.W., 2005. Mean free-path length theory of predator–prey interactions: application to juvenile salmon migration. *Ecol. Modell.* 186, 196–211.
- Anderson, J.J., Spring 2002. An agent-based event driven foraging model. *Nat. Resour. Modell.* 15 (1).
- Anderson, J.J., 2000a. A vitality-based model relating stressors and environmental properties to organism survival. *Ecol. Monogr.* 70 (3), 445–470.
- Anderson, J.D., 2000b. Modeling impacts of multiple stresses on aquatic ecosystems: case study of juvenile Chinook salmon in the Sacramento River system. Ph.D. dissertation. Department of Civil and Environmental Engineering, University of California at Davis, Davis, California.
- Anderson, J.J., 1991. Fish bypass system mathematical models. In: Proceedings from ASCE Waterpower '91, Denver, CO, July 24–26.
- Anderson, J.J., 1988. Diverting migrating fish past turbines. *Northwest Environ. J.* 4, 109–128.
- Anglea, S.M., Ham, K.D., Johnson, G.E., Simmons, M.A., Simmons, C.S., Kudera, E., Skalski, J.R., 2003. Hydroacoustic evaluation of the removable spillway weir at Lower Granite Dam in 2002. Final report prepared by Battelle Pacific Northwest Division for U.S. Army Corps of Engineers, Walla Walla District, Walla Walla, WA.
- Anglea, S.M., Johnson, R.L., Simmons, M.A., Thorsten, S.L., Duncan, J.P., Chamness, M.A., McKinstry, C.A., Kudera, E.A., Skalski, J.R., 2001. Fixed-location hydroacoustic evaluation of the prototype surface bypass and collector at Lower Granite Dam in 2000. Final report prepared by Battelle Pacific Northwest Division for U.S. Army Corps of Engineers, Walla Walla District, Walla Walla, WA.
- Backman, T.W.H., Evans, A.F., Robertson, M.S., 2002. Gas bubble trauma incidence in juvenile salmonids in the lower Columbia and Snake Rivers. *North Am. J. Fish. Manage.* 22, 965–972.
- Bart, J., 1995. Acceptance criteria for using individual-based models to make management decisions. *Ecol. Appl.* 5 (2), 411–420.
- Beamish, F.W.H., 1978. In: Hoar, W.S., Randall, D.J. (Eds.), *Fish Physiology Volume VII "Locomotion"*. Academic Press, New York, NY, pp. 101–183.
- Bian, L., 2003. The representation of the environment in the context of individual-based modeling. *Ecol. Modell.* 159, 279–296.
- Birtwell, I.K., Korstrom, J.S., Brotherston, A.E., 2003. Laboratory studies on the effects of thermal change on the behaviour and distribution of juvenile chum salmon in sea water. *J. Fish Biol.* 62, 85–96.
- Bourque, M.-C., LeBlond, P.H., Cummins, P.F., 1999. Effects of tidal currents on Pacific salmon migration: results from a fine-resolution coastal model. *Can. J. Fish. Aquat. Sci.* 56, 839–846.
- Braun, C.B., Coombs, S., 2000. The overlapping roles of the inner ear and lateral line: the active space of dipole source detection. *Philos. Trans. R. Soc. Lond. Ser. B* 355 (1401), 1115–1119.
- Brett, J.R., 1952. Temperature tolerance in young Pacific salmon, genus *Oncorhynchus*. *J. Fish. Res. Board Can.* 9, 265–323.
- Bult, T.P., Riley, S.C., Haedrich, R.L., Gibson, R.J., Heggenes, J., 1999. Density dependent habitat selection by juvenile Atlantic salmon (*Salmo salar*) in experimental riverine habitats. *Can. J. Fish. Aquat. Sci.* 56, 1298–1306.
- Bush, R.R., Mosteller, R., 1955. *Stochastic Models for Learning*. Wiley, New York, NY.

- Cash, K.M., Adams, N.S., Hatton, T.W., Jones, E.C., Rondorf, D.W., 2002. Three-dimensional fish tracking to evaluate the operation of the Lower Granite surface bypass collector and behavioral guidance structure during 2000. Final report prepared by U.S. Geological Survey Columbia River Research Laboratory for the U.S. Army Corps of Engineers, Walla Walla District, Walla Walla, WA.
- Cheng, J.-R., Jones, M., Plassmann, P.E., 2004. A portable software architecture for mesh-independent particle tracking algorithms. *J. Parallel Algorithms Appl.* 19 (2–3), 145–161.
- Cheng, J.-R., Plassmann, P.E., 2004. A parallel particle tracking framework for applications in scientific computing. *J. Supercomput.* 28 (2), 149–164.
- Cheng, J.-R., Plassmann, P.E., 2002. A parallel algorithm for the dynamic partitioning of particle-mesh computational systems. *Computational Science—ICCS 2002. The Springer-Verlag Lecture Notes in Computer Science (LNCS 2331) series, Part III*, pp. 1020–1029.
- Cheng, J.-R., Plassmann, P.E., 2001. The accuracy and performance of parallel in-element particle tracking methods. In: *Proceedings of the 10th SIAM Conference on Parallel Processing for Scientific Computing*, Portsmouth, VA, March, pp. 252–261.
- Christie, C.G., Regier, H.A., 1988. Measurements of optimal habitat and their relationship to yields for four commercial fish species. *Can. J. Fish. Aquat. Sci.* 45, 301–314.
- Clark, M.E., Rose, K.A., 1997. Individual-based model of stream-resident rainbow trout and brook char: model description, corroboration, and effects of sympatry and spawning season duration. *Ecol. Modell.* 94, 157–175.
- Coombs, S., 1999. Signal detection theory, lateral-line excitation patterns and prey capture behaviour of mottled sculpin. *Anim. Behav.* 58, 421–430.
- Coombs, S., 1996. Interepore spacings on canals may determine distance range of lateral line system. *Soc. Neurosci. Abstr.* 22, 1819.
- Coombs, S., Braun, C.B., Donovan, B., 2001. The orienting response of Lake Michigan mottled sculpin is mediated by canal neuromasts. *J. Exp. Biol.* 204, 337–348.
- Coombs, S., Finneran, J.J., Conley, R.A., 2000. Hydrodynamic image formation by the peripheral lateral line system of the Lake Michigan mottled sculpin, *Cottus bairdi*. *Philos. Trans. R. Soc. Lond. Ser. B* 355 (1401), 1111–1114.
- Costa, M., Ferreira, J.S., 2000. Discrete particle distribution model for advection-diffusion transport. *ASCE J. Hydraul. Eng.* 126 (7), 525–532.
- Coutant, C.C., 2001. Integrated, multi-sensory, behavioral guidance systems for fish diversions. In: Coutant, C.C. (Ed.), *Behavioral Technologies for Fish Guidance*. American Fisheries Society, Symposium, vol. 26, Bethesda, MD, pp. 105–113.
- Coutant, C.C., 1987. Thermal preference: when does an asset become a liability? *Environ. Biol. Fish.* 18, 161–172.
- Coutant, C.C., Whitney, R.R., 2000. Fish behavior in relation to passage through hydropower turbines: a review. *Trans. Am. Fish. Soc.* 129, 351–380.
- Dagorn, L., Menczer, F., Bach, P., Olson, R.J., 2000. Co-evolution of movement behaviours by tropical pelagic predatory fishes in response to prey environment: a simulation model. *Ecol. Modell.* 134, 325–341.
- DeAngelis, D.L., Cushman, R.M., 1990. Potential applications of models in forecasting the effects of climate change on fisheries. *Trans. Am. Fish. Soc.* 119, 224–239.
- Denton, E.J., Gray, J.A., 1983. Mechanical factors in the excitation of clupeid lateral lines. *Proc. R. Soc. Lond. Ser. B* 218, 1–26.
- Denton, E.J., Gray, J.A., 1988. Mechanical factors in the excitation of the lateral line of fishes. In: Atema, J., Fay, R.R., Popper, A.N., Tavolga, W.N. (Eds.), *Sensory Biology of Aquatic Animals*. Springer, New York, NY, pp. 595–617.
- Denton, E.J., Gray, J.A., 1989. Some observations on the forces acting on neuromasts in fish lateral line canals. In: Coombs, S., Görner, P., Münz, H. (Eds.), *The Mechanosensory Lateral Line: Neurobiology and Evolution*. Springer-Verlag, New York, NY, pp. 229–246.
- Dunning, J.B., Stewart, D.J., Danielson, B.J.N.R., Noon, B.R., Root, T.R., Lamberson, R.H., Stevens, E.E., 1995. Spatially explicit population models: current forms and future uses. *Ecol. Appl.* 5, 3–11.
- Ewing, B., Yandell, B.S., Barbieri, J.F., Luck, R.F., Forster, L.D., 2002. Event-driven competing risks. *Ecol. Modell.* 158, 35–50.
- Faber, D.M., Hanks, M.E., Zimmerman, S.A., Skalski, J.R., Dillingham, P., 2004. The Distribution and Flux of Fish in the Forebay of The Dalles Dam in 2003 and Implications for Surface Flow Bypass. Draft final report prepared for the U.S. Army Engineer District, Portland by Battelle Pacific Northwest National Laboratories, Richland, WA.
- Gaff, H., DeAngelis, D.L., Gross, L.J., Salinas, R., Shorosh, M., 2000. A dynamic landscape model for fish in the Everglades and its application to restoration. *Ecol. Modell.* 127, 33–52.
- Gerolotto, F., Soria, M., Fréon, P., 1999. From two dimensions to three: The use of multi-beam sonar for a new approach to fisheries acoustics. *Can. J. Fish. Aquat. Sci.* 56 (1), 6–12.
- Ginot, V., Le Page, C., Souissi, S., 2002. A multi-agents architecture to enhance end-user individual-based modelling. *Ecol. Modell.* 157, 23–41.
- Goodwin, R.A., 2004. Hydrodynamics and juvenile salmon movement behavior at Lower Granite Dam: decoding the relationship using 3-D space-time (CEL Agent IBM) simulation. Ph.D. Dissertation. Cornell University, Ithaca, NY.
- Goodwin, R.A., Nestler, J.M., Loucks, D.P., Chapman, R.S., 2001. Simulating mobile populations in aquatic ecosystems. *J. Water Resour. Plann. Manage.* 127 (6), 386–393.
- Grimm, V., Wyzomirski, T., Aikman, D., Uchmański, J., 1999. Individual-based modeling and ecological theory: synthesis of a workshop. *Ecol. Modell.* 115, 275–282.
- Haefner, J.W., Bowen, M.D., 2002. Physical-based model of fish movement in fish extraction facilities. *Ecol. Modell.* 152, 227–245.
- Halle, S., Halle, B., 1999. Modelling activity synchronization in free-ranging microtine rodents. *Ecol. Modell.* 115, 165–176.
- Hanna, R.B., Saito, L., Bartholow, J.M., Sandelin, J., 1999. Results of simulated temperature control device operations on in-reservoir and discharge water temperatures using CE-QUAL-W2. *J. Lake Reserv. Manage.* 15 (2), 87–102.
- Harte, J., 2002. Toward a synthesis of the Newtonian and Darwinian worldviews. *Phys. Today* 55 (10), 29.

- Hastings, A., Palmer, M.A., 2003. A bright future for biologists and mathematicians? *Science* 299, 2003–2004.
- Hills, T.T., Adler, F.R., 2002. Time's crooked arrow: optimal foraging and rate-biased time perception. *Anim. Behav.* 64, 589–597.
- Hinckley, S., Hermann, A.J., Megrey, B.A., 1996. Development of a spatially explicit, individual-based model of marine fish early life history. *Mar. Ecol. Progr. Ser.* 139, 47–68.
- Hinrichsen, H.-H., Möllmann, C., Voss, R., Köster, F.W., Kornilovs, G., 2002. Biophysical modeling of larval Baltic cod (*Gadus morhua*) growth and survival. *Can. J. Fish. Aquat. Sci.* 59, 1858–1873.
- Hirvonen, H., Ranta, E., Rita, H., Peuhkuri, N., 1999. Significance of memory properties in prey choice decisions. *Ecol. Modell.* 115, 177–189.
- Hudspeth, A.J., 1989. How the ear's works work. *Nature* 341, 397–404.
- Hussko, A., Vuorimies, O., Sutela, T., 1996. Temperature- and light-mediated predation by perch on vendace larvae. *J. Fish Biol.* 49, 441–457.
- Huth, A., Wissel, C., 1994. The simulation of fish schools in comparison with experimental data. *Ecol. Modell.* 75/76, 135–145.
- Huth, A., Wissel, C., 1992. The simulation of the movement of fish shoals. *J. Theor. Biol.* 156, 365–385.
- Ijspeert, A.J., Kodjabachian, J., 1999. Evolution and development of a central pattern generator for the swimming of a lamprey. *Artif. Life* 5, 247–269.
- Jager, H.I., Rose, K.A., 2003. Designing optimal flow patterns for fall Chinook salmon in a Central Valley, California, river. *North Am. J. Fish. Manage.* 23, 1–21.
- Johnson, P.N., Kim, J., 2004. Review and Synthesis of Juvenile Salmonid Distributions in the Forebay of Lower Granite Dam. Draft letter report prepared for the US Army Engineer Research and Development Center, Vicksburg, MS.
- Johnson, G.E., Hedgepeth, J., Giorgi, A., Skalski, J., 2000. Evaluation of smolt movements using an active fish tracking sonar at the sluiceway surface bypass, The Dalles Dam, 2000. Draft final report, U.S. Army Corps of Engineers, Portland District, Portland, OR.
- Johnson, R.L., Anglea, S.M., Blanton, S.L., Simmons, M.A., Moursund, R.A., Johnson, G.E., Kudrea, E.A., Thomas, J., Skalsik, J.R., 1999. Hydroacoustic Evaluation of Fish Passage and Behavior at Lower Granite Dam in Spring 1998. Final report prepared for U.S. Army Engineer District, Walla Walla by Battelle Pacific Northwest National Laboratories, Richland, WA.
- Kalmijn, A.J., 2000. Detection and processing of electromagnetic and near-field acoustic signals in elasmobranch fishes. *Philos. Trans. R. Soc. Lond. Ser. B* 355 (1401), 1135–1141.
- Kalmijn, A.J., 1989. Functional evolution of lateral line and inner-ear sensory systems. In: Coombs, S., Görner, P., Münz, H. (Eds.), *The Mechanosensory Lateral Line: Neurobiology and Evolution*. Springer-Verlag, New York, NY, pp. 187–215.
- Kalmijn, A.J., 1988. Hydrodynamic and acoustic field detection. In: Atema, J., Fay, R.R., Popper, A.N., Tavolga, W.N. (Eds.), *Sensory Biology of Aquatic Animals*. Springer, New York, NY, pp. 83–130.
- Karim, M.R., Sekine, M., Higuchi, T., Imai, T., Ukita, M., 2003. Simulation of fish behavior and mortality in hypoxic water in an enclosed bay. *Ecol. Modell.* 159, 27–42.
- Khoshniat, M., Stuhne, G.R., Steinman, D.A., 2003. Relative performance of geometric search algorithms for interpolating unstructured mesh data. In: *The Sixth Annual International Conference on Medical Image Computing and Computer Assisted Intervention (MICCAI)*, Montreal, November.
- Kondolf, G.M., Larsen, E.W., Williams, J.G., 2000. Measuring and modeling the hydraulic environment for assessing instream flows. *North Am. J. Fish. Manage.* 20, 1016–1028.
- Kröther, S., Mogdans, J., Bleckmann, H., 2002. Brainstem lateral line responses to sinusoidal wave stimuli in still and running water. *J. Exp. Biol.* 205, 1471–1484.
- Lai, Y.G., Weber, L.J., Patel, V.C., 2003a. Nonhydrostatic three-dimensional model for hydraulic flow simulation. I. Formulation and Verification. *J. Hydraulic Eng.* 129 (3), 196–205.
- Lai, Y.G., Weber, L.J., Patel, V.C., 2003b. Nonhydrostatic three-dimensional model for hydraulic flow simulation. II: Validation and Application. *J. Hydraulic Eng.* 129 (3), 206–214.
- Lai, Y.G., 2000. Unstructured grid arbitrarily shaped element method for fluid flow simulation. *AIAA J.* 38 (12), 2246–2252.
- LGL Limited, 2005. Analysis of smolt behavior and relative survival at Wanapum Dam using three-dimensional acoustic telemetry, 2004. Prepared in conjunction with Hydroacoustic Technology, Inc. for Public Utility District No. 2 of Grant County, January 19, 2005.
- Loucks, D.P., van Beek, E., 2005. *Water Resource Systems Planning and Management, Methods, Models and Applications*. UNESCO Press, Paris, France.
- Loucks, D.P., Stedinger, J.R., Haith, D.A., 1981. *Water Resource Systems Planning and Analysis*. Prentice-Hall, Englewood Cliffs, NJ.
- Lucas, M.C., Baras, E., 2000. Methods for studying spatial behaviour of freshwater fishes in the natural environment. *Fish. Fish.* 1, 283–316.
- Mahesh, K., Constantinescu, S.G., Moin, P., 2004. A numerical method for large eddy simulation in complex geometries. *J. Comput. Phys.* 197 (1), 215–240.
- Marsh, L.M., Jones, R.E., 1988. The form and consequences of random walk movement models. *J. Theor. Biol.* 133, 113–131.
- McCoy, A., Constantinescu, S.G., Weber, L., 2005. LES simulation of contaminant removal from the embayment area between two vertical groynes in a channel. In: *XXXIst International Association Hydraulic Research Congress*, Seoul, Korea, September.
- Monte, L., 2002. A methodology for modelling the contamination of moving organisms in water bodies with spatial and time dependent pollution levels. *Ecol. Modell.* 158, 21–33.
- Montgomery, J.C., Carton, A.G., Voigt, R., Baker, C.F., Diebel, C., 2000. Sensory processing of water currents by fishes. *Philos. Trans. R. Soc. Lond. Ser. B* 355 (1401), 1325–1327.
- Montgomery, J.C., Coombs, S., Halstead, M., 1995. Biology of the mechanosensory lateral line in fishes. *Rev. Fish Biol. Fish.* 5, 399–416.
- Moursund, R.A., Ham, K.D., Titzler, P.S., Khan, F., 2003. Hydroacoustic evaluation of the effects of spill treatments on fish passage at Ice Harbor Dam in 2003. Draft final report prepared by Battelle

- Pacific Northwest Division for U.S. Army Corps of Engineers, Walla Walla District, Walla Walla, WA.
- Nestler, J.M., Goodwin, R.A., Loucks, D.P., 2005. Coupling of engineering and biological models for ecosystem analysis. *J. Water Resour. Plann. Manage.* 131 (2), 101–109.
- Nestler, J.M., Goodwin, R.A., Cole, T., Degan, D., Dennerline, D., 2002. Simulating movement patterns of blueback herring in a stratified southern impoundment. *Trans. Am. Fish. Soc.* 131, 55–69.
- New, J.G., Fewkes, L.A., Khan, A.N., 2001. Strike feeding behavior in the muskellunge, *Esox masquinongy*: contributions of the lateral line and visual sensory systems. *J. Exp. Biol.* 204, 1207–1221.
- Niwa, H.S., 1994. Self-organizing dynamic model of fish schooling. *J. Theor. Biol.* 171, 123–136.
- Nonacs, P., Smith, P.E., Bouskila, A., Luttbeg, B., 1994. Modeling the Behavior of the Northern Anchovy, *Engraulis mordax*, as a Schooling Predator Exploiting Patchy Prey. *Deep-Sea Res. II*, 41(1). Elsevier Science Ltd, Great Britain, pp. 147–169.
- Parrish, J.K., Edelman-Keshet, L., 1999. Complexity, pattern, and evolutionary trade-offs in animal aggregation. *Science* 284, 99–101.
- Paxton, J.R., 2000. Fish otoliths: do sizes correlate with taxonomic group, habitat and/or luminescence? *Philos. Trans. R. Soc. Lond. Ser. B* 355 (1401), 1299–1303.
- Pelletier, D., Parma, A.M., 1994. Spatial distribution of Pacific halibut (*Hippoglossus stenolepis*): an application of geostatistics to longline survey data. *Can. J. Fish. Aquat. Sci.* 51, 1506–1518.
- Petersen, J.H., DeAngelis, D.L., 2000. Dynamics of prey moving through a predator field: a model of migrating juvenile salmon. *Math. Biosci.* 165, 97–114.
- Pientka, B., Parrish, D.L., 2002. Habitat selection of predator and prey: Atlantic salmon and rainbow smelt overlap, based on temperature and dissolved oxygen. *Trans. Am. Fish. Soc.* 131, 1180–1193.
- Plumb, J.M., Braatz, A.C., Lucchesi, J.N., Fielding, S.D., Cochran, A.D., Nation, T.K., Sprando, J.M., Schei, J.L., Perry, R.W., Adams, N.S., Rondorf, D.W., 2004. Behavior and survival of radio-tagged juvenile chinook salmon and steelhead relative to the performance of a removable spillway weir at Lower Granite Dam, Washington, 2003. Final report prepared by U.S. Geological Survey Columbia River Research Laboratory for the U.S. Army Corps of Engineers, Walla Walla District, Walla Walla, WA.
- Popper, A.N., Carlson, T.J., 1998. Application of sound and other stimuli to control fish behavior. *Trans. Am. Fish. Soc.* 127, 673–707.
- Prairie, Y.T., 1996. Evaluating the predictive power of regression models. *Can. J. Fish. Aquat. Sci.* 53, 490–492.
- Railsback, S., 1999. Reducing uncertainties in instream flow studies. *Fisheries* 24 (4), 24–26.
- Railsback, S.F., Lamberson, R.H., Harvey, B.C., Duffy, W.E., 1999a. Movement rules for individual-based models of stream fish. *Ecol. Modell.* 123, 73–89.
- Railsback, S.F., Lamberson, R.H., Jackson, S., 1999b. Individual-based models: progress toward viability for fisheries management. In: *Presentation at Spatial Processes and Management of Fish Populations*, 17th Lowell Wakefield Symposium, Anchorage, Alaska.
- Reese, C.D., Harvey, B.C., 2002. Temperature-dependent interactions between juvenile steelhead and Sacramento pikeminnow in laboratory streams. *Trans. Am. Fish. Soc.* 131, 599–606.
- Reuter, H., Breckling, B., 1994. Selforganization of fish schools: an object-oriented model. *Ecol. Modell.* 75/76, 147–159.
- Romey, W.L., 1996. Individual differences make a difference in the trajectories of simulated schools of fish. *Ecol. Modell.* 92, 65–77.
- Rogers, P.H., Cox, M., 1988. Underwater sound as a biological stimulus. In: Atema, J., Fay, R.R., Popper, A.N., Tavolga, W.N. (Eds.), *Sensory Biology of Aquatic Animals*. Springer, New York, NY, pp. 131–149.
- Scheibe, T.D., Richmond, M.C., 2002. Fish individual-based numerical simulator (FINS): a particle-based model of juvenile salmonid movement and dissolved gas exposure history in the Columbia River basin. *Ecol. Modell.* 147, 233–252.
- Schilt, C.R., Nestler, J.M., 1997. Fish bioacoustics: considerations for hydropower industry workers. In: *Proceedings of the International Conference on Hydropower*, Atlanta, GA, August 5–8.
- Schindler, D.E., Eby, L.A., 1997. Stoichiometry of fishes and their prey: implications for nutrient recycling. *Ecology* 78 (6), 1816–1831.
- Schmalz, P.J., Hansen, M.J., Holey, M.E., McKee, P.C., Toney, M.L., 2002. Lake Trout movements in northwestern Lake Michigan. *North Am. J. Fish. Manage.* 22, 737–749.
- Smith, E.P., Rose, K.A., 1995. Model goodness-of-fit analysis using regression and related techniques. *Ecol. Modell.* 77, 49–64.
- Smith, S.G., Muir, W.D., Williams, J.G., Skalski, J.R., 2002. Factors associated with travel time and survival of migrant yearling Chinook salmon and Steelhead in the lower Snake River. *North Am. J. Fish. Manage.* 22, 385–405.
- Sogard, S.M., Olla, B.L., 1993. Effects of light, thermoclines and predator presence on vertical distribution and behavioral interactions of juvenile walleye pollock, *Theragra chalcogramma* Pallas. *J. Exp. Mar. Biol. Ecol.* 167, 179–195.
- Stedinger, J.R., 2000. The use of risk and uncertainty analyses within the US Army Corps of Engineers Civil Works Programs. Prepared for USACE Institute for Water Resources by Cornell University, Ithaca, NY.
- Steel, E.A., Guttorp, P., Anderson, J.J., Caccia, D.C., 2001. Modeling juvenile migration using a simple Markov chain. *J. Agric. Biol. Environ. Stat.* 6 (1), 80–88.
- Steig, T.W., 1999. The use of acoustic tags to monitor the movement of juvenile salmonids approaching a dam on the Columbia River. In: *Proceedings of the 15th International Symposium on Biotelemetry*, Juneau, AK, 9–14 May.
- Steig, T.W., Johnson, W.R., 1986. Hydroacoustic assessment of downstream migrating salmonids at The Dalles Dam in spring and summer 1985. Final Report DOE/BP-23174-2, U.S. Department of Energy, Bonneville Power Administration, Portland, OR.
- Stockwell, J.D., Johnson, B.M., 1997. Refinement and calibration of a bioenergetics-based foraging model for kokanee (*Oncorhynchus nerka*). *Can. J. Fish. Aquat. Sci.* 54 (11), 2659–2676.

- Terzopoulos, D., Tu, X., Grezeszczuk, R., 1995. Artificial fishes: autonomous locomotion, perception, behavior, and learning in a simulated physical world. *Artif. Life* 1, 327–351.
- Tischendorf, L., 1997. Modelling individual movements in heterogeneous landscapes: potentials of a new approach. *Ecol. Modell.* 103, 33–42.
- Tokyay, T., Constantinescu, S.G., 2005. Large eddy simulation and Reynolds averaged Navier–Stokes simulations of flow in a realistic pump intake: a validation study. In: *World Water and Environmental Resources Congress*, Anchorage, Alaska, May.
- Turchin, P., 1998. *Quantitative Analysis of Movement*. Sinauer Assoc, Sunderland, MA.
- van Nes, E.H., Lammens, E.H.R.R., Scheffer, M., 2002. PISCATOR, an individual-based model to analyze the dynamics of lake fish communities. *Ecol. Modell.* 152, 261–278.
- Van Winkle, W., Rose, K.A., Chambers, R.C., 1993. Individual-based approach to fish population dynamics: an overview. *Trans. Am. Fish. Soc.* 122, 397–403.
- Van Winkle, W., Jager, H.I., Railsback, S.F., Holcomb, B.D., Studley, T.K., Baldrige, J.E., 1998. Individual-based model for sympatric populations of brown and rainbow trout for instream flow assessment: model description and calibration. *Ecol. Modell.* 110, 175–207.
- Voigt, R., Carton, A.G., Montgomery, J.C., 2000. Responses of anterior lateral line afferent neurons to water flow. *J. Exp. Biol.* 203, 2495–2502.
- Weber, E.H., 1846. Der Tastsinn und das Gemeingefühl. In: Wagner, R. (Ed.), *Handwörterbuch der Physiologie*. Braunschweig, Bieweg.
- Workman, R.D., Hayes, D.B., Coon, T.G., 2002. A model of steelhead movement in relation to water temperature in two Lake Michigan tributaries. *Trans. Am. Fish. Soc.* 131, 463–475.
- Wu, H., Li, B.-L., Springer, T.A., Neill, W.H., 2000. Modelling animal movement as a persistent random walk in two dimensions: expected magnitude of net displacement. *Ecol. Modell.* 132, 115–124.
- Xiao, Y., 2000. An individual-based approach to evaluating experimental designs for estimating rates of fish movement from tag recoveries. *Ecol. Modell.* 128, 149–163.